
Electronic Thesis and Dissertation Repository

12-13-2022 3:00 PM

A Novel Passive Islanding Detection Method Based on Phase-Locked Loop

Hoda Zamani, *The University of Western Ontario*

Supervisor: Ajaei, Firouz B, *The University of Western Ontario*

A thesis submitted in partial fulfillment of the requirements for the Master of Engineering Science degree in Electrical and Computer Engineering

© Hoda Zamani 2022

Follow this and additional works at: <https://ir.lib.uwo.ca/etd>



Part of the [Electrical and Electronics Commons](#), and the [Power and Energy Commons](#)

Recommended Citation

Zamani, Hoda, "A Novel Passive Islanding Detection Method Based on Phase-Locked Loop" (2022). *Electronic Thesis and Dissertation Repository*. 9038.
<https://ir.lib.uwo.ca/etd/9038>

This Dissertation/Thesis is brought to you for free and open access by Scholarship@Western. It has been accepted for inclusion in Electronic Thesis and Dissertation Repository by an authorized administrator of Scholarship@Western. For more information, please contact wlsadmin@uwo.ca.

Abstract

The ever-increasing penetration of distributed energy resources in power distribution systems has led to challenges in the detection of islanding. Among different islanding detection methods (IDMs), passive methods are the least intrusive and typically require the lowest investment cost. However, they generally suffer from larger non-detection zones (NDZs) and higher nuisance detection ratios as compared to active, hybrid, and remote IDMs. This study provides an overview of the criteria outlined in the existing technical literature for the performance evaluation of IDMs, a review and comparison of the existing passive IDMs, and an analysis of the phase-locked loop (PLL) behaviour under grid-connected and islanded conditions using its quasi-static model. Based on the results of these studies, a novel passive IDM is developed that utilizes the PLL error to detect islanding with a small NDZ and high speed.

The performance of the proposed IDM is evaluated under various islanding and non-islanding disturbances. The performance evaluation studies are conducted through simulations in the PSCAD software environment as well as experimental tests using a hybrid microgrid test platform. The study results indicate that the proposed method: *(i)* can detect islanding in less than two cycles, which is well below the requirements of the IEEE 1547 standard, *(ii)* leads to a small NDZ and can identify islanding with only $\pm 5\%$ power mismatch, *(iii)* does not cause false detection of non-islanding disturbances as islanding, and *(iv)* is robust against noise.

Keywords: Islanding detection, distributed energy resources, non-detection zone, phase-locked loop

Summary for Lay Audience

Under normal conditions, the utility grid and distributed energy resources (DERs) operate in parallel to supply power to consumers. If for any reason (e.g., a fault) an upstream circuit breaker opens and disconnects a DER from the rest of the grid, an island may form where the DER continues to feed the adjacent loads without the voltage and frequency support from the grid. Unintentional islanding must be rapidly detected since it leads to safety hazards for utility workers and maintenance personnel.

There are several categories of islanding detection techniques such as passive and active methods. A desirable islanding detection scheme is dependable, secure, robust, fast, cost-effective and non-intrusive. None of the existing islanding detection approaches meets all these requirements. For instance, active methods are generally reliable but degrade power quality. In contrast, passive methods do not adversely affect the power quality but may fail to detect islanding in some cases. This thesis introduces a novel passive islanding detection method which is fast and inexpensive. It operates reliably under most islanding/non-islanding scenarios and does not require communication systems. The proposed method is evaluated and validated through both simulation studies and experimental tests.

To Behnam.

For his advice, his patience, and his faith.

And because he always understood.

Acknowledgments

I would like to express my sincerest gratitude to my supervisor, Dr. Firouz Badrkhani Ajaei, for his unwavering support and understanding, and for bringing the weight of his considerable experience and knowledge to this project. His high expectations have made me better at what I do.

I would also like to deeply thank the examination committee, Dr. Rajiv Varma, Dr. Dennis Michaelson, and Dr. Hamidreza Abdolvand, for their great consideration and constructive comments.

I wish to express my special thanks to my friend and coworker, Sina Driss, for his kindhearted help and for his great work in building the *Hybrid Microgrid Test Platform* which was used in this research.

Finally, I would like to wholeheartedly thank my beloved family, Payiz and Homa. Without them, none of this would indeed be possible.

Table of Contents

Abstract.....	ii
Summary for Lay Audience	iii
Acknowledgments	v
Table of Contents.....	vi
List of Tables	ix
List of Figures.....	x
List of Abbreviations	xv
Chapter 1.....	1
1 Introduction	1
1.1 Background	1
1.2 Statement of the Problem.....	6
1.3 Research Objectives	6
1.4 Methodology	7
1.5 Study Systems	8
1.5.1 Study System 1: Canadian Benchmark Rural Distribution Network.....	8
1.5.2 Study System 2: IEEE Recommended Test System for Islanding Detection Studies	10
1.5.3 Study System 3: Hybrid Microgrid Test Platform.....	11
1.6 Contributions	13
Chapter 2.....	14

2 Literature Review	14
2.1 Criteria for Performance Evaluation of IDMs	14
2.1.1 Non-Detection Zone.....	14
2.1.2 Detection Time Delay	17
2.1.3 Applicability in Multi-DER Systems.....	17
2.1.4 Nuisance Detection Ratio	17
2.1.5 Effect on Power Quality and Stability	18
2.1.6 Cost	18
2.2 Review of the Existing Passive IDMs.....	19
2.2.1 Conventional Passive IDMs.....	19
2.2.2 Signal Processing-Based IDMs.....	22
2.2.3 Artificial Intelligence-Based IDMs.....	25
2.3 Summary and Conclusions.....	29
Chapter 3.....	32
3 The Proposed Islanding Detection Method.....	32
Chapter 4.....	38
4 Performance Evaluation	38
4.1 Islanding.....	39
4.1.1 Non-Detection Zone.....	42
4.1.2 Detection Time.....	56
4.2 Non-Islanding Disturbances	58

4.2.1 Fault ‘F1’	58
4.2.2 Fault ‘F2’	60
4.2.3 Motor Starting	62
4.2.4 Static Load Switching	66
4.2.5 Nuisance Detection	69
Chapter 5	70
5 Conclusions	70
5.1 Conclusions	70
5.2 Future Work	72
References.....	73
Appendices	94
Curriculum Vitae	99

List of Tables

Table 1: Islanding Detection Requirements According to IEEE Recommended Practices.....	11
Table 2: High-Level Comparison of Islanding Detection Methods.....	31
Table 3: NDZ of the Investigated IDMs.....	55
Table 4: Detection Time of the Investigated IDMs.....	56
Table 5: Nuisance Detection in the Investigated IDMs.	69

List of Figures

Figure 1.1: Categories of islanding detection methods.	3
Figure 1.2: Study system 1: Canadian benchmark rural distribution network.	9
Figure 1.3: Study system 2: recommended test system for islanding detection studies according to IEEE 1547-2018 and IEEE 929-2000 recommended practice.....	10
Figure 1.4: Study system 3: hybrid microgrid test platform: (a) single-line diagram, and (b) the implemented hardware.....	12
Figure 2.1: NDZ representation in the power mismatch space.....	15
Figure 2.2: Structure of an artificial neural network.....	26
Figure 2.3: Structure of a decision tree classifier.....	28
Figure 2.4: Number of the research papers published between 1992-2021 in each category of IDMs.....	30
Figure 3.1: Structure of the SRF PLL.	33
Figure 3.2: Quasi-static PLL model.	34
Figure 3.3: Flowchart of the proposed IDM.....	37
Figure 4.1: Variations of different operating quantities utilized for passive islanding detection under an islanding event in the study system 1, at $t = 0.2$ s (simulation results): (a) PCC voltage magnitude, (b) frequency, (c) ROCOV, (d) ROCOF, (e) ROCOP, and (f) q-axis voltage V_q	40
Figure 4.2: Variations of different operating quantities utilized for passive islanding detection under islanding event in the study system 3, at $t = 0.2$ s (experimental results): (a) PCC voltage magnitude, (b) frequency, (c) ROCOF, (d) ROCOV, (e) ROCOP, and (f) q-axis voltage V_q	41

Figure 4.3: Variations of different operating quantities utilized for passive islanding detection under an islanding event in the study system 2, at $t = 0.2$ s, considering a -15% power mismatch (simulation results): (a) PCC voltage magnitude, (b) frequency, (c) ROCOV, (d) ROCOF, (e) ROCOP, and (f) q-axis voltage Vq43

Figure 4.4: Variations of different operating quantities utilized for passive islanding detection under an islanding event in the study system 2, at $t = 0.2$ s, considering a $+15\%$ power mismatch (simulation results): (a) PCC voltage magnitude, (b) frequency, (c) ROCOV, (d) ROCOF, (e) ROCOP, and (f) q-axis voltage Vq44

Figure 4.5: Variations of different operating quantities utilized for passive islanding detection under an islanding event in the study system 2, at $t = 0.2$ s, considering a -10% power mismatch (simulation results): (a) PCC voltage magnitude, (b) frequency, (c) ROCOV, (d) ROCOF, (e) ROCOP, and (f) q-axis voltage Vq46

Figure 4.6: Variations of voltage magnitude under an islanding event considering a -10% power mismatch (left) and the generated IDS (right), zoomed-in version of Figure 4.5 (a).47

Figure 4.7: Variations of different operating quantities utilized for passive islanding detection under an islanding event in the study system 2, at $t = 0.2$ s, considering a $+10\%$ power mismatch (simulation results): (a) PCC voltage magnitude, (b) frequency, (c) ROCOV, (d) ROCOF, (e) ROCOP, and (f) q-axis voltage Vq48

Figure 4.8: Variations of different operating quantities utilized for passive islanding detection under an islanding event in the study system 2, at $t = 0.2$ s, considering a -5% power mismatch (simulation results): (a) PCC voltage magnitude, (b) frequency, (c) ROCOV, (d) ROCOF, (e) ROCOP, and (f) q-axis voltage Vq50

Figure 4.9: Variations of frequency under an islanding event considering a -5% power mismatch (left) and the generated IDS (right), zoomed-in version of Figure 4.8 (b).51

Figure 4.10: Variations of different operating quantities utilized for passive islanding detection under an islanding event in the study system 2, at $t = 0.2$ s, considering a $+5\%$ power mismatch (simulation results): (a) PCC voltage magnitude, (b) frequency, (c) ROCOV, (d) ROCOF, (e) ROCOP, and (f) q-axis voltage Vq52

Figure 4.11: Variations of q-axis voltage Vq under an islanding event considering a $+5\%$ power mismatch (left) and the generated IDS (right), zoomed-in version of Figure 4.10 (f).53

Figure 4.12: Variations of different operating quantities utilized for passive islanding detection under an islanding event in the study system 2, at $t = 0.2$ s, considering a 0% power mismatch (simulation results): (a) PCC voltage magnitude, (b) frequency, (c) ROCOV, (d) ROCOF, (e) ROCOP, and (f) q-axis voltage Vq54

Figure 4.13: Variations of different operating quantities utilized for passive islanding detection under fault ‘F1’ in the study system 1, at $t = 0.2$ s (simulation results): (a) PCC voltage magnitude, (b) frequency, (c) ROCOV, (d) ROCOF, (e) ROCOP, and (f) q-axis voltage Vq59

Figure 4.14: Variations of frequency under fault ‘F1’ (left) and the generated IDS (right), zoomed-in version of Figure 4.13 (b).60

Figure 4.15: Variations of different operating quantities utilized for passive islanding detection under fault ‘F2’ in study system 1, at $t = 0.2$ s (simulation results): (a) PCC voltage magnitude, (b) frequency, (c) ROCOV, (d) ROCOF, (e) ROCOP, and (f) q-axis voltage Vq61

Figure 4.16: Variations of different operating quantities utilized for passive islanding detection under motor starting in the study system 1, at $t = 0.2$ s (simulation results): (a) PCC voltage magnitude, (b) frequency, (c) ROCOV, (d) ROCOF, (e) ROCOP, and (f) q-axis voltage Vq63

Figure 4.17: Variations of different operating quantities utilized for passive islanding detection under motor starting in the study system 3, at $t = 0.2$ s (experimental results): (a) PCC voltage magnitude, (b) frequency, (c) ROCOF, (d) ROCOV, (e) ROCOP, and (f) q-axis voltage Vq64

Figure 4.18: Variations of voltage magnitude under motor starting (left) and the generated IDS (right), zoomed-in version of Figure 4.17 (a).65

Figure 4.19: Variations of different operating quantities utilized for passive islanding detection under static load switching in the study system 1, at $t = 0.2$ s (simulation results): (a) PCC voltage magnitude, (b) frequency, (c) ROCOV, (d) ROCOF, (e) ROCOP, and (f) q-axis voltage Vq67

Figure 4.20: Variations of different operating quantities utilized for passive islanding detection under static load switching in the study system 3, at $t = 0.2$ s (experimental results): (a) PCC voltage magnitude, (b) frequency, (c) ROCOF, (d) ROCOV, (e) ROCOP, and (f) q-axis voltage Vq68

List of Appendices

Appendix A: Study System 1 Parameters	94
Appendix B: Study System 3 Parameters.....	97

List of Abbreviations

DER	Distributed Energy Resource
PV	Photovoltaic
WT	Wind Turbine
BESS	Battery Energy Storage System
PCC	Point of Common Coupling
IDM	Islanding Detection Method
NDZ	Non-Detection Zone
UOV	Under/Over Voltage
UOF	Under/Over Frequency
ROCOV	Rate of Change of Voltage
ROCOF	Rate of Change of Frequency
ROCOP	Rate of Change of Power
PLL	Phase-Locked Loop
PMSG	Permanent Magnet Synchronous generator
HHT	Hilbert Huang Transform
ACF	Auto-Correlation Function
ANN	Artificial Neural Network
PNN	Probabilistic Neural Network
SRF	Synchronous Reference Frame
IDS	Islanding Detection Signal
FD	False Detection

Nomenclature

Q_f	Load quality factor
R	Equivalent lumped load resistance
L	Equivalent lumped load inductance
C	Equivalent lumped load capacitance
V_n	System nominal voltage
f_n	System nominal frequency
P_{Load}	Load active power
V_q	q-axis component of PCC voltage
ΔP	Generation-load active power mismatch
ΔQ	Generation-load reactive power mismatch
C_{norm}	Normalized capacitance
f_0	Load resonant frequency
V_d	d-axis component of PCC voltage
$v_a, v_b, \text{ and } v_c$	Instantaneous voltages of phase a, b, and c
ω'	Angular frequency tracked by PLL
V_{grid}	Grid voltage amplitude
I_{inv}	Inverter current amplitude reference
φ_{inv}	phase shift angle due to the presence of the reactive components in the load and grid impedances
z_L	Local load impedance
z_g	Grid impedance
ω	Grid angular frequency
K_1	Grid synchronization loop gain
K_2	Self synchronization loop gain

θ	PCC phase angle
θ'	Phase angle tracked by PLL
v^-	Grid synchronization loop voltage
v^+	Self synchronization loop voltage
R_f	Fault resistance

Chapter 1

1 Introduction

1.1 Background

Distributed energy resources (DERs) are dispersed power generation units, e.g., photovoltaic (PV) systems and wind turbines (WTs), or energy storage units like battery energy storage systems (BESSs), that are integrated into the distribution systems [1], [2].

The utility grid and DERs work in parallel to supply the local load. Islanding is defined as a condition in which a portion of the utility system is energized by DERs while it is electrically separated from the rest of the utility grid [3]–[5]. This phenomenon can be intentional or unintentional [6], [7]. Intentional islanding is a controlled event that is typically triggered for scheduled operations such as system maintenance, while unintentional islanding happens due to unforeseen events such as faults and other disturbances in the power system [8].

Unintentional islanding must be detected with high speed and reliability to minimize safety hazards and prevent equipment damage [4], [9]. The

challenges posed by unintentional islanding include but are not limited to [10], [11]:

- Health hazards for utility workers who may not be aware that the line is energized by DER(s).
- Unsynchronized reconnection of the island to the grid may result in excessively large currents and damage to the DERs. Also, it may cause protective relays to trip.

Islanding detection methods (IDMs) can be broadly categorized into local and remote techniques [12]–[15], as shown in Figure 1.1. Remote IDMs [16]–[20] rely on communication between the utility grid and the DERs to provide zero non-detection zone (NDZ), meaning they are capable of islanding detection even with perfect generation-load power balance. However, remote IDMs are costly due to the required communication systems [12], [14], [21] and suffer from the risk of communication failure. Local IDMs, which do not utilize remote communication, are further divided into passive, active, and hybrid methods [12]–[14].

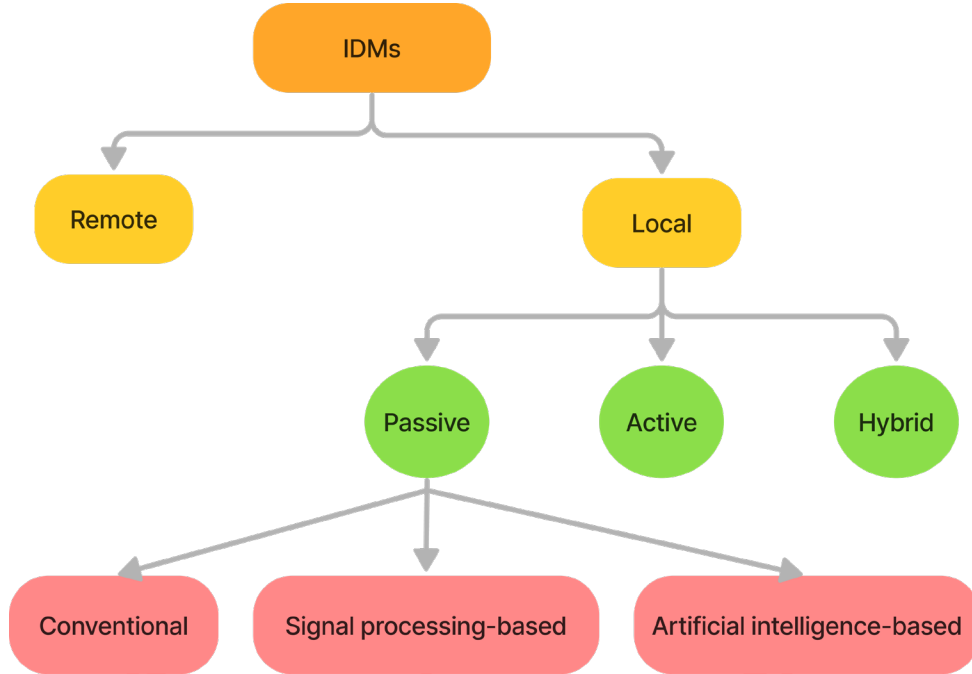


Figure 1.1: Categories of islanding detection methods.

Passive methods [22]–[27] monitor system parameters such as voltage and frequency and compare them with pre-determined thresholds to detect islanding [28]. An advantage of passive IDMs is that they do not degrade power quality. The conventional passive methods are simple, cost-effective, easy to implement, and independent of DER control strategies. However, the existing conventional passive IDMs generally suffer from a large NDZ, i.e., may fail to detect islanding when there is a small generation-load power mismatch [27], [29], [30].

Signal processing-based [31]–[33] and artificial intelligence-based techniques [34]–[36] are other categories of IDMs that are considered as improved

passive methods [4], [37], [38]. Although the improved passive IDMs have alleviated some of the shortcomings of the conventional passive techniques, they generally suffer from increased cost and complexity, high computational burden, and in some cases noise sensitivity [21], [39].

An active IDM [40]–[44] forces a specific system parameter to deviate and exceed the corresponding thresholds by injecting a perturbation signal [4], [30]. Active IDMs benefit from small NDZs but may adversely affect power quality and system stability [45], [46], suffer from low speed [29], [47], and become less effective in systems with multiple DERs [21], [48].

In a hybrid IDM [13], [49]–[51], active islanding detection is enabled only when islanding is suspected by the passive scheme [26], [52]. Hybrid IDMs benefit from less power quality degradation as compared to active IDMs but do not eliminate the power quality and stability issues of active methods [46].

Among the existing passive IDMs, those operating based on under/over voltage (UOV) [5], [53], under/over frequency (OUF) [5], [9], [53], [54], rate of change of voltage (ROCOV) [14], [55], rate of change of frequency (ROCOF) [56]–[58], and rate of change of power (ROCOP) [14], [59] are the most widely used [9], [60]. These methods are prone to false detection due to faults and load fluctuations [61], [62] and are not able to detect islanding when

the generation and load are closely matched [25], [30], [62], [63]. However, if the shortcoming of large NDZ is overcome, passive methods can be suitable candidates for practical applications owing to their simplicity and cost-effectiveness [27], [64]. A more detailed review of the existing passive IDMs is presented in Chapter 2.

Several studies [65]–[68] have proposed to utilize the deviation of phase-locked loop (PLL) output (i.e., frequency) during islanding to detect islanding. However, frequency-based islanding detection is not always reliable. In addition, most of the studies have not used any models for the prediction of PLL behaviour under islanded conditions and thus, they lack design procedures and generalizability.

1.2 Statement of the Problem

As discussed in part 1.1, active IDMs degrade power quality and may suffer from low speed. Also, they are not reliable methods for islanding detection of multi-DER systems. On the other hand, the existing passive IDMs either suffer from large NDZs or are computationally expensive and sensitive to noise. This requires the development of a simple and robust IDM. The high costs associated with remote IDMs limit their practical application. Therefore, there is a need to develop a fast and reliable IDM that is cost-effective, does not degrade power quality, does not require communication, and can be applied to multi-DER systems.

1.3 Research Objectives

The objectives of this research are (i) developing a passive IDM with high speed, high reliability, and a small NDZ, (ii) devising a systematic approach for setting the parameters of the proposed method, and (iii) verifying the acceptable performance of the proposed IDM under various islanding and non-islanding scenarios through simulation studies and experimental tests.

1.4 Methodology

The methodology to achieve the above-mentioned objectives includes:

- Developing an algorithm to detect islanding based on the variations of the PLL error.
- Verifying the acceptable performance of the proposed IDM in grid-connected inverters through time-domain simulation of the Canadian benchmark medium-voltage distribution system [69]–[71] in the PSCAD software environment.
- Determining the NDZ of the proposed IDM according to the procedures outlined in IEEE 1547-2018 [3] and IEEE 929-2000 [72] in the PSCAD software environment.
- Investigating the performance of the proposed IDM under practical conditions through experimental tests using a microgrid test platform.
- Evaluating and comparing the performance of the proposed IDM with those of the five most commonly used passive IDMs, which operate based on UOV, UOF, ROCOF, ROCOV, and ROCOP.

1.5 Study Systems

The following subsections describe the utilized study systems and their roles in the evaluation of the proposed IDM.

1.5.1 Study System 1: Canadian Benchmark Rural Distribution Network

A detailed and realistic model of the modified Canadian benchmark rural distribution network [69]–[71], including the switching models of the converters and the associated control systems, is utilized for simulation studies in the PSCAD software environment. The study system 1 includes a 3.5 MW PV generation unit, a 4 MW wind power plant composed of two 2 MW permanent magnet synchronous generator (PMSG)-based WTs, and two 2 MW BESSs¹, as shown in Figure 1.2. The study system 1 is used for the performance evaluation of the proposed IDM, including the detection time and nuisance detection ratio². For a fair comparison between the IDMs, the results of the time-domain simulation studies in PSCAD are used to choose the best set of parameters for the investigated passive IDMs.

¹ Refer to Appendix A for the parameters.

² Refer to Chapter 2 for the definitions.

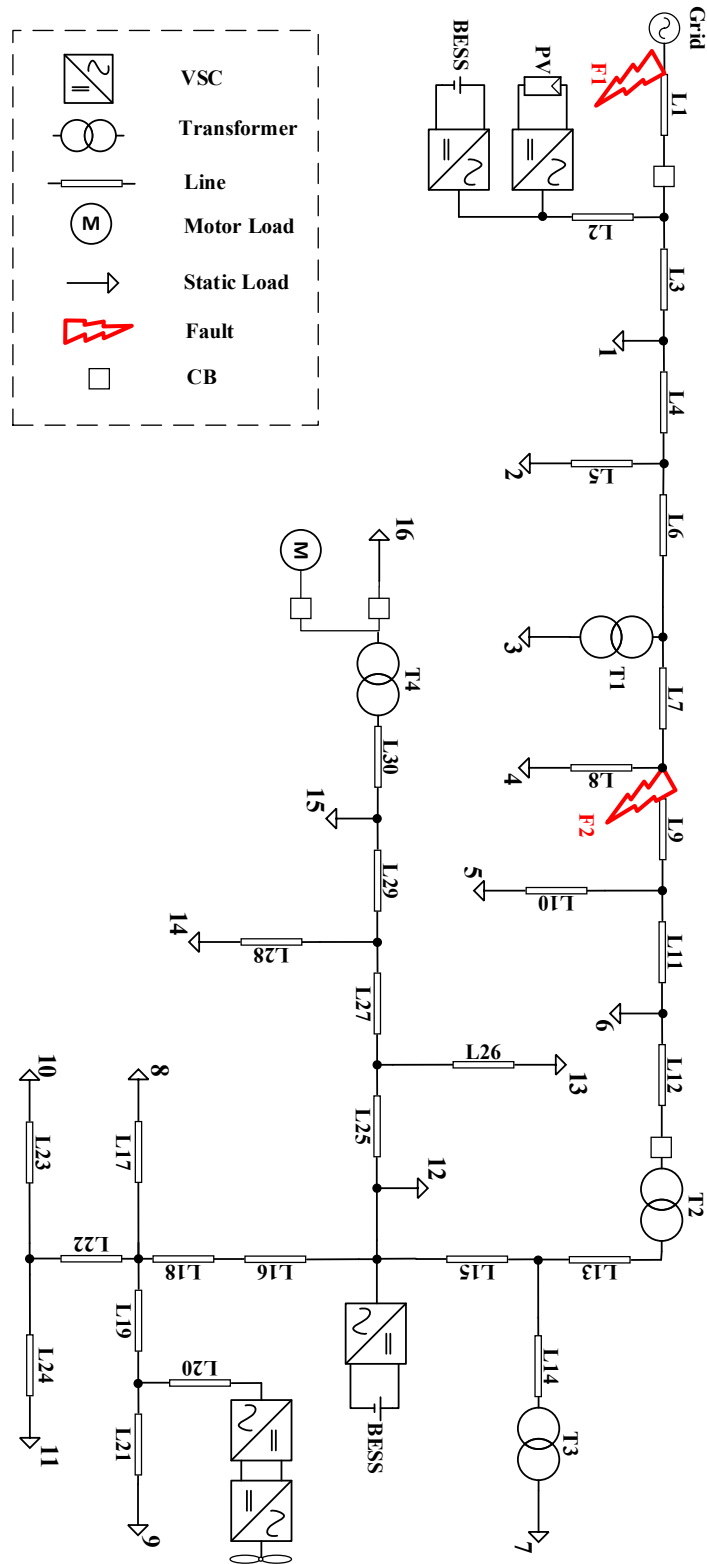


Figure 1.2: Study system 1: Canadian benchmark rural distribution network.

1.5.2 Study System 2: IEEE Recommended Test System for Islanding Detection Studies

One of the most widely utilized references for islanding detection requirements of DERs is the IEEE 1547-2018 standard [3]. IEEE 929-2000 [72] also provides recommended practices for the utility interface of PV systems. The test system illustrated in Figure 1.3 is a simplified representation of an islanded system, which is recommended by IEEE 1547 and IEEE 929 for the investigation of NDZ.

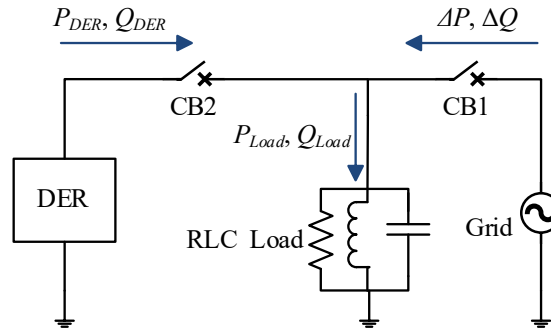


Figure 1.3: Study system 2: recommended test system for islanding detection studies according to IEEE 1547-2018 and IEEE 929-2000 recommended practice.

The study system of Figure 1.3 is used for identifying the NDZ of the IDMs under different generation-load power mismatches. The islanding detection requirements outlined in [3] and [72] are summarized in Table 1. The quality factor Q_f in Table 1 describes the aggregate load within the islanded system, which is represented by a parallel RLC branch (as shown in Figure 1.3) to consider the most difficult scenario for islanding detection [8], [73].

Table 1: Islanding Detection Requirements According to IEEE Recommended Practices.

	IEEE 1547-2018	IEEE 929-2000
Quality factor	1	2.5
Detection time	$t < 2 \text{ s}$	$t < 2 \text{ s}$
Normal frequency range	$59.3 \text{ Hz} \leq f \leq 60.5 \text{ Hz}$	$59.3 \text{ Hz} \leq f \leq 60.5 \text{ Hz}$
Normal voltage range	$88\% \leq V \leq 110\%$	$88\% \leq V \leq 110\%$

The test system equivalent load parameters R , L , and C can be calculated as:

$$R = \frac{V_n^2}{P_{Load}} \quad (1)$$

$$L = \frac{V_n^2}{2\pi f_n Q_f P_{Load}} \quad (2)$$

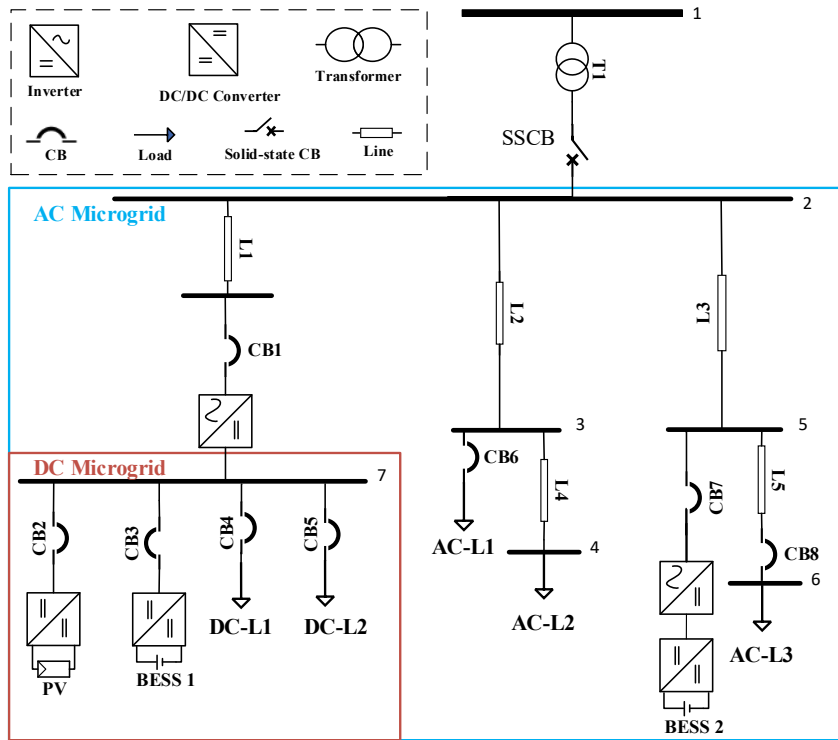
$$C = \frac{Q_f P_{Load}}{2\pi f_n V_n^2} \quad (3)$$

where P_{Load} is the load active power, and V_n and f_n are the system nominal voltage and frequency, respectively.

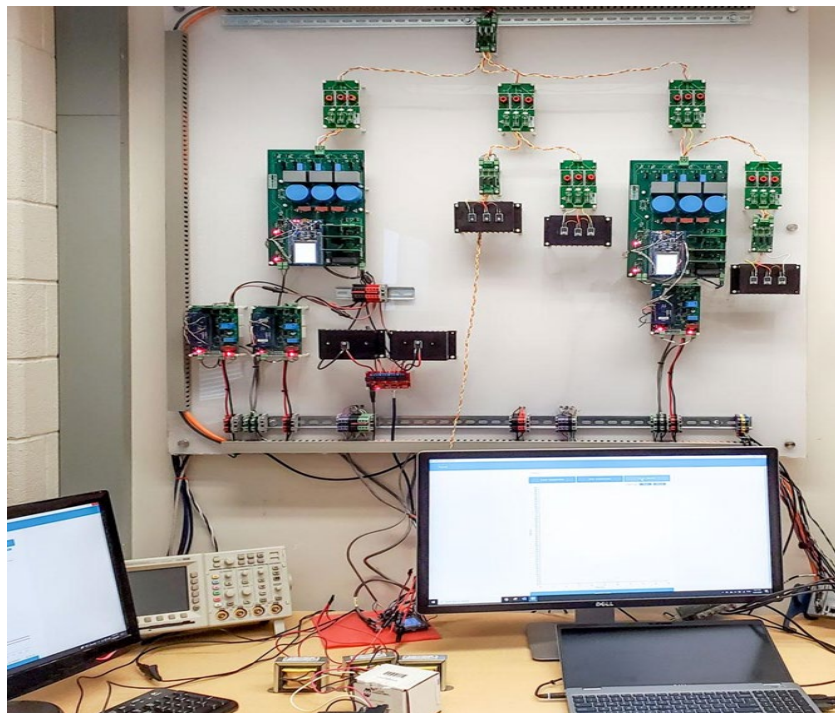
1.5.3 Study System 3: Hybrid Microgrid Test Platform

Study system 3 is a hardware-implemented hybrid microgrid which is used for experimental validation of the proposed passive IDM. This system utilizes a 40 V DC bus and a 16 V three-phase AC bus¹ as shown in Figure 1.4.

¹ Refer to Appendix B for the parameters.



(a)



(b)

Figure 1.4: Study system 3: hybrid microgrid test platform: (a) single-line diagram, and (b) the implemented hardware.

1.6 Contributions

The main contributions of this thesis are listed below.

- The proposed IDM is capable of islanding detection within 2 cycles, which is faster than the requirements of IEEE 1547.
- The parameters of the proposed IDM can be systematically determined for any specific system.
- The NDZ of the proposed method is small as compared to most of the existing passive IDMs while it does not adversely affect power quality and stability and does not require costly computation and communication systems.
- The proposed IDM does not cause false detection of non-islanding events as islanding.
- The proposed method is reliable, i.e., dependable and secure.

Chapter 2

2 Literature Review

In this chapter, first, the criteria for the performance evaluation of IDMs are described. Then, a review of the existing passive IDMs is provided, and finally, a high-level comparison of the existing IDMs is presented.

2.1 Criteria for Performance Evaluation of IDMs

Several criteria are used to determine how reliably and fast an IDM can detect islanding. These criteria include NDZ, detection time, applicability in multi-DER systems, nuisance detection ratio, effect on power quality and stability, and cost.

2.1.1 Non-Detection Zone

The most important indicator in the evaluation of IDMs is the NDZ. It is defined as the operating region of an IDM in which islanding cannot be detected. The aforementioned operating region can be described in either power mismatch space or load parameter space [62], [73], [74].

2.1.1.1 NDZ in the Power Mismatch Space

Under islanded operating conditions, if the DER power output and the load power within the islanded system of Figure 1.3 are closely matched, the variations in voltage and frequency caused by islanding will not be sufficiently large to be detected. The worst-case scenario in the detection of islanding happens when there is no generation-load power mismatch, i.e., $\Delta P = 0$ and $\Delta Q = 0$ [73], [75].

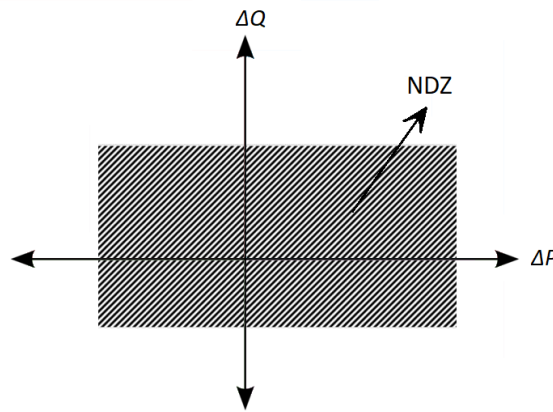


Figure 2.1: NDZ representation in the power mismatch space.

The power mismatch space describes the range of active and reactive power mismatches (ΔP versus ΔQ) which do not cause the system variables to exceed the corresponding thresholds [48], [62], as depicted in Figure 2.1. The power mismatch space is an effective indicator of NDZ for passive IDMs [48], [74].

2.1.1.2 NDZ in the Load Parameter Space

The NDZ of an active frequency drifting method is typically evaluated using the load parameter space [73], [74]. In this method, the DER and load active powers are assumed to be matched, i.e., $\Delta P = 0$. Using (1)-(3), the equivalent load parameters (R , L , and C) are determined. The load parameter space maps the NDZ of an IDM into C_{norm} versus L space [76]. C_{norm} is defined as the ratio of the load capacitance to the capacitance that resonates with the load inductance at the grid frequency and is given by:

$$C_{norm} = \frac{C}{C_{res}} = C\omega^2 L \quad (4)$$

One drawback of the C_{norm} versus L space is that different values of R lead to different NDZs in the load parameter space. This issue is addressed in [77] by proposing Q_f versus f_0 load parameter space instead, where f_0 is the load resonant frequency and Q_f is the load quality factor which can be expressed as:

$$Q_f = R \sqrt{\frac{C}{L}} \quad (5)$$

2.1.2 Detection Time Delay

Detection time is the time elapsed from the occurrence of islanding to the time instant at which islanding is detected. Fast detection of islanding conditions is necessary to minimize the adverse effects of unintentional islanding [73].

2.1.3 Applicability in Multi-DER Systems

An island in a modern power system may comprise not only more than one DER but also multiple types of DERs. The effectiveness of IDMs may decrease in the multi-DER case, e.g., where multiple inverters rely on power output variation for active islanding detection. As more inverters are added, the unsynchronized alteration of the outputs may lead to an insignificant change in system variables and failure to detect islanding [73], [78].

2.1.4 Nuisance Detection Ratio

IDMs should not detect non-islanding disturbances such as faults and load switching events as islanding. The nuisance detection ratio is defined as the ratio of the number of false detection cases to the total number of islanding detection cases [62]. An excessively sensitive IDM has a small NDZ but is likely to have a high nuisance detection ratio.

2.1.5 Effect on Power Quality and Stability

IDMs based on perturbation injection, i.e., active or hybrid, degrade the power quality during islanding and may even trigger instability [38], [62]. Therefore, IDMs with minimum effect on power quality are preferred.

2.1.6 Cost

Implementation of some IDMs requires the installation of costly hardware which can limit their practical application. A compromise between cost and performance must be made for real-world applications [73].

2.2 Review of the Existing Passive IDMs

This section provides a review of the existing passive IDMs. In the following parts, the different types of passive IDMs are discussed.

2.2.1 Conventional Passive IDMs

The existing conventional passive IDMs can be categorized into different groups based on the system variables utilized to detect islanding, including UOV, UOF, ROCOV, ROCOF, ROCOP, harmonic detection, voltage unbalance, phase jump detection, and vector shift. The most widely used conventional passive IDMs are discussed below.

2.2.1.1 Under/Over Voltage and Under/Over Frequency

The OUV and OUF protective elements are typically used in grid-connected PV inverters [30], [79]. These elements monitor voltage and frequency at the point of common coupling (PCC) and compare them with pre-determined thresholds. In an islanded system, the voltage and frequency deviations are indicators of the active and reactive power mismatches, i.e., ΔP and ΔQ in Figure 1.3 [39], [80], and thus enable islanding detection. Islanding detection based on OUV is simple and cost-effective but suffers from large NDZ, meaning small power mismatches may not cause sufficient deviations in the

voltage to exceed the corresponding thresholds. The UOV- and UOF-based IDMs generally suffer from a high nuisance detection ratio. Therefore, these passive IDMs are used as backup protection against unintentional islanding [53], [62], [81].

2.2.1.2 Rate of Change of Voltage

The ROCOV can be used to detect islanding conditions as the variations of the PCC voltage during islanding are typically larger than normal [30], [37], [82]. However, non-islanding events such as motor starting and capacitor bank switching can also cause the ROCOV to exceed the threshold and lead to nuisance detection [14].

2.2.1.3 Rate of Change of Frequency

The ROCOF has been widely utilized for passive islanding detection. Upon islanding, the generation-load power imbalance causes frequency deviation and leads to a large ROCOF. Protective relays operating based on the ROCOF measure the time derivative of frequency over a few cycles to detect islanding [30], [62], [83]. This method requires a generation-load power mismatch of more than 15% to reliably detect islanding [81], [84], [85] and may suffer from low detection speed [57], [86], [87].

2.2.1.4 Rate of Change of Power

After an islanding incident, the ROCOP measured by each DER at its terminal is typically greater than the ROCOP under normal conditions. Islanding can be detected when the rate of change of the DER output power exceeds a threshold [80], [88]. A disadvantage of the ROCOP-based IDM is that it may cause nuisance detection if the DER output power changes too fast under normal operating conditions [81].

2.2.2 Signal Processing-Based IDMs

A group of passive IDMs utilize signal processing techniques to extract features from power system variables, e.g., voltage, frequency, and ROCOF, that can be used for the detection of islanding. The most commonly used signal processing tools are the wavelet transform, S-transform, and Hilbert Huang transform (HHT) [39], [73]. These techniques are briefly discussed below.

The wavelet transform is a linear transformation similar to the Fourier transform but with better time-localization of signal frequency components. This technique has been utilized in a variety of power system applications [89]. The wavelet transform-based IDM extracts the energy coefficients of the power system signals. It detects islanding if the extracted energy coefficients exceed certain thresholds. Wavelet suffers from a high computational burden and noise sensitivity [81].

An extension of the concept of the wavelet transform is S-transform [39], [90]. In [91] a method using wavelet transform and S-transform is proposed to extract features for the detection of islanding and power quality disturbances. The findings of [92], [93] indicate that the performance of the wavelet transform degrades considerably under noisy situations, while S-transform

can perform reliably under both noise-free and noisy conditions. A disadvantage of the S-transform is that its performance degrades under certain conditions such as power system transients [73], [94], [95].

The HHT is a powerful signal processing tool that is developed based on empirical mode decomposition and Hilbert transform [96]. The advantages of the HHT as a robust signal processing technique over the wavelet transform and S-transform have been demonstrated in the literature [97]–[100]. The findings of [101] indicate that the HHT can be utilized for islanding detection with a small NDZ and is applicable to multi-DER systems. However, HHT requires a long time to process a signal [102].

Mathematical morphology is a relatively simple signal processing technique based on the addition and subtraction of signals [73], [103]. The studies reported in [104], [105] indicate that mathematical morphology enables fast islanding detection under a variety of operating conditions, e.g., noise. However, this method tends to remove important features from noisy data along with the noise [106].

The auto-correlation function (ACF) is a signal processing technique that represents the correlation between a signal and its delayed version, which is used to extract hidden information from signals [39], [107]. ACF is used in [107], [108], and the results show that it leads to a small NDZ. As compared to other signal processing-based IDMs, ACF is computationally efficient. However, it may lead to false detection of non-islanding events [109].

The Kalman filter is a famous time-frequency domain signal processing technique that has been used to extract features such as harmonics from power system signals [39], [47]. The results of the studies conducted on the application of the Kalman filter for islanding detection as well as other power system applications indicate that this method performs reliably in noisy environments and is less sensitive to harmonics as compared to wavelet transform [47], [110]–[112]. However, the Kalman filter is complex and computationally expensive [113].

2.2.3 Artificial Intelligence-Based IDMs

There are difficulties associated with the threshold selection for conventional and signal processing-based passive IDMs. If the threshold is chosen with a large safety margin, the IDM becomes less sensitive and may fail to detect islanding. If the threshold is chosen without a sufficient safety margin, the IDM becomes too sensitive and may cause nuisance detection. Artificial intelligence-based IDMs operate based on various system parameters, e.g., voltage, frequency, ROCOF, and ROCOP, that can indicate islanding, without requiring the user to determine the thresholds [30], [73], [81]. These IDMs discriminate islanding from other operating conditions through pattern recognition and event classification. There are several intelligent classifiers such as artificial neural network (ANN) [114]–[118], probabilistic neural network (PNN) [119], [120], artificial immune system [121], [122], decision tree [123]–[126], and fuzzy logic [127]–[131], which are employed to rapidly detect islanding. The most common techniques are discussed below.

As one of the most widely used intelligent classifiers for power system applications, ANNs consist of input, hidden, and output layers with connected neurons, as shown in Figure 2.2. ANNs mimic the behaviour of the human brain. It is shown in [30], [117] that the ANN can detect islanding with high

speed even when the load quality factor Q_f is large. In [132], ANN is used for fast islanding detection with high accuracy. However, ANN has certain disadvantages. The learning process may not achieve a high accuracy due to the multi-modal nature of the data. Furthermore, the generalizability of the ANN-IDM is a concern because its performance relies on the utilized neural network architecture.

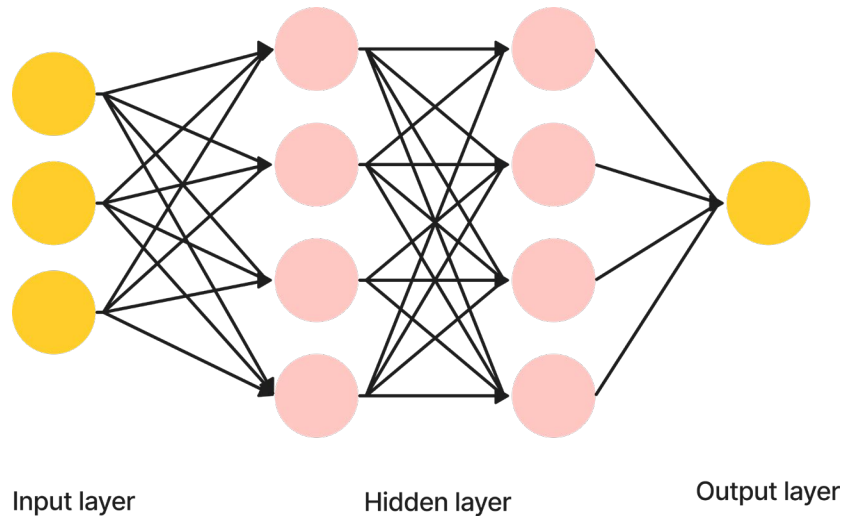


Figure 2.2: Structure of an artificial neural network.

The PNN is a type of neural network with fast training capability that is essentially developed based on the Bayesian function. The PNN classifier is utilized in [133] for islanding detection, where the features extracted by wavelet transform are fed to a PNN classifier for the detection of islanding events. An average accuracy of 89.76% is achieved which is too low. PNNs generally require more computational resources and time than ANNs.

The decision tree is another intelligent classification technique that can break a complex decision-making process into several simpler decisions by using splitting criteria [134], [135]. As shown in Figure 2.3, the splits are made on decision nodes based on splitting criteria. A leaf node is where no more splits are made. The decision tree classifier and the wavelet transform have been used together in [124], which has led to an islanding detection accuracy of 98%. An advantage of decision trees as compared to other pattern recognition methods is a faster training process, but it has limitations such as complexity and the dependence of the islanding detection threshold on the splitting criteria [30], [35], [39], [73].

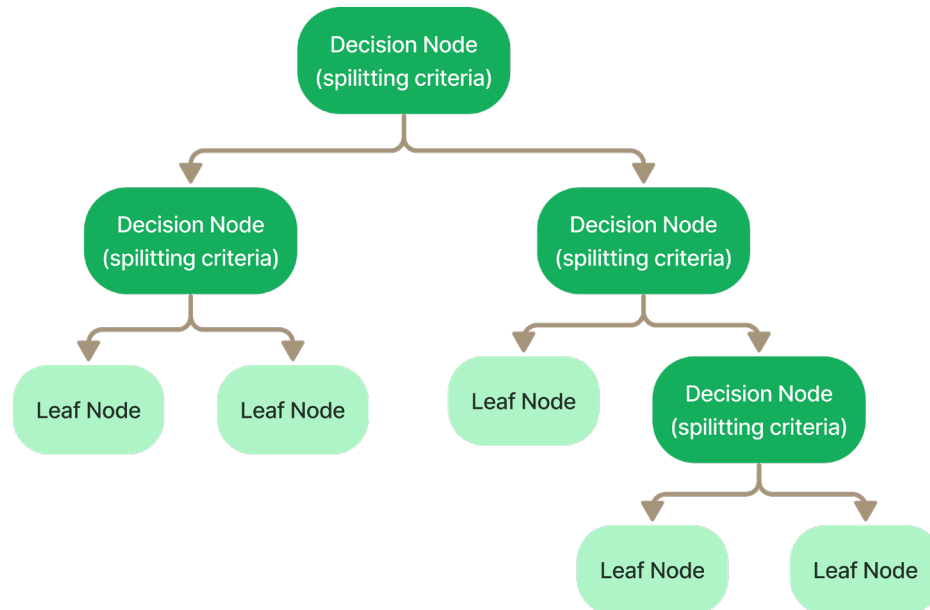


Figure 2.3: Structure of a decision tree classifier.

Fuzzy logic is considered a promising tool for modelling ambiguity, uncertainty, and imprecision in a mathematical form [30]. In [131], the features extracted by S-transform are fed into a fuzzy rule-based classifier to detect islanding, where the average accuracy of 99.8% is achieved. An advantage of fuzzy rule-based classifiers as compared to decision trees is better interpretability [131]. However, it suffers from some shortcomings such as sensitivity to noise, lack of self-organization and self-tuning mechanisms, and a need for expert knowledge [30], [39], [129], [136].

2.3 Summary and Conclusions

The advantages and disadvantages of each category of IDMs are briefly outlined in part 1.1. All categories of IDMs have some advantages and disadvantages; there is no existing IDM that can outperform other methods in all performance indices and operate impeccably under all scenarios.

The main disadvantage of the conventional passive IDMs is their relatively large NDZ. To tackle the shortcomings associated with conventional passive IDMs, the application of signal processing and artificial intelligence in islanding detection has received significant attention. However, the challenges associated with their higher cost, computational burden, and noise sensitivity still need to be addressed.

The number of the research papers published between 1992-2021 is presented in Figure 2.4 which is obtained from the research information datasets available in *IEEE Xplore*¹, *Google Scholar*², and *Dimensions*³. The research trend in islanding detection studies suggest an encouraging future for passive IDMs.

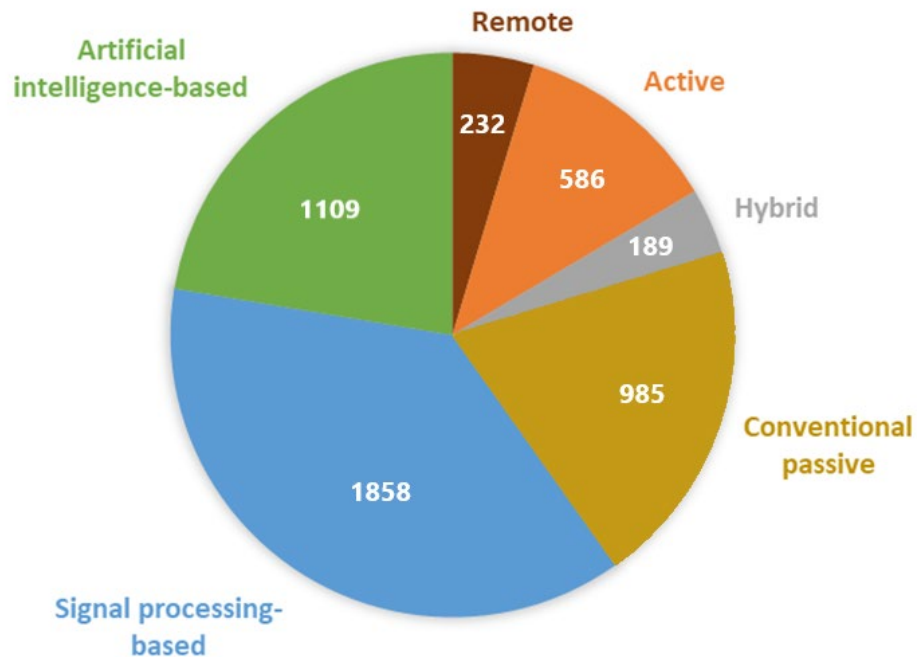


Figure 2.4: Number of the research papers published between 1992-2021 in each category of IDMs.

¹ <https://ieeexplore.ieee.org/search/advanced>

² <https://scholar.google.com/>

³ <https://app.dimensions.ai/discover/publication>

Table 2 provides a high-level comparison of the passive, active, hybrid, and remote IDMs.

Table 2: High-Level Comparison of Islanding Detection Methods.

Classification of IDMs		Principle of operation	NDZ	Detection speed	Effect on power quality	Cost	Applicability in multi-DER systems
Passive	Conventional	Monitoring changes in system parameters	Large	High	None	Low	Preferred
	Signal processing-based	Feature extraction	Negligible	High	None	High	Preferred
	Artificial intelligence-based	Pattern recognition	Negligible	High	None	High	Preferred
Active		Perturbation	Small	Low	Highly degrades power quality	Medium	Not preferred
Hybrid		Combination of passive and active methods	Small	Medium	Degrades power quality	Medium	Not preferred
Remote		Communication b/w DER and utility	Zero	Medium	None	Very high	Preferred

Chapter 3

3 The Proposed Islanding Detection Method

Accurate detection of the frequency and phase angle of the grid voltage is one of the basic requirements for the interconnection of DERs with the utility grid, for which a PLL is widely used [137], [138]. Typically, a PLL consists of three components, namely a phase detector, a loop filter, and a digitally controlled oscillator [139]–[141]. The main difference among the PLLs is in the implementation of the phase detector [140]–[142].

Synchronous reference frame (SRF) PLLs which use DQ transformation as the phase detector [141] are widely utilized in three-phase systems [138], [140], [141]. Figure 3.1 shows the structure of the SRF PLL. The three-phase voltages measured at the PCC undergo DQ transformation in a rotating frame which results in the following signals:

$$V_d = \frac{2}{3}(v_a \sin(\omega't) + v_b \sin(\omega't - 2\pi/3) + v_c \sin(\omega't + 2\pi/3)) \quad (6)$$

$$V_q = \frac{2}{3}(v_a \cos(\omega't) + v_b \cos(\omega't - 2\pi/3) + v_c \cos(\omega't + 2\pi/3)) \quad (7)$$

where v_a , v_b , and v_c are the PCC instantaneous voltages of phase a , b , and c respectively, and ω' is the frequency tracked by the PLL. The lock is realized by controlling the q-axis component of voltage (V_q), i.e., the PLL error to be zero, which is achieved using a PI regulator.

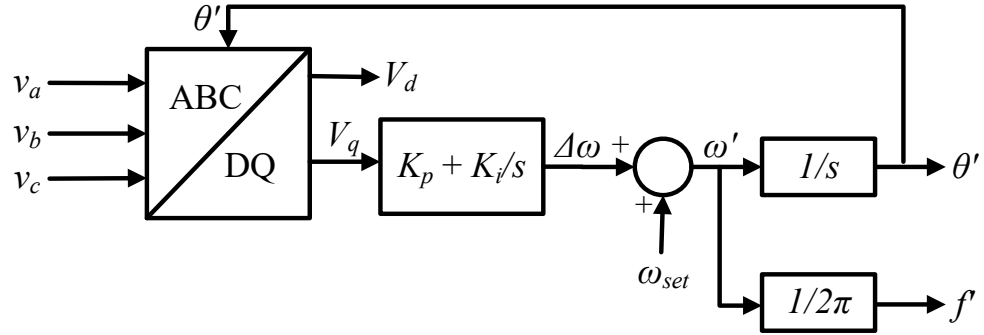


Figure 3.1: Structure of the SRF PLL.

In [141], a quasi-static PLL model is proposed which can be used for the analysis of the PLL behaviour in an islanded system. The quasi-static model consists of the self synchronization loop and the grid synchronization loop, as shown in Figure 3.2. In this model, V_{grid} is the grid voltage amplitude, I_{inv} is the inverter current amplitude reference, and $\varphi_{inv}(\omega')$ is the phase shift angle due to the presence of the reactive components in the local load and the grid impedance, as shown in (8) [141].

$$\varphi_{inv}(\omega') = \angle \left(\frac{z_L(\omega')z_g(\omega')}{z_L(\omega') + z_g(\omega')} \right) \quad (8)$$

In (8), $z_L(\omega')$ and $z_g(\omega')$ are the local load equivalent impedance and the grid impedance both at the tracked frequency, respectively.

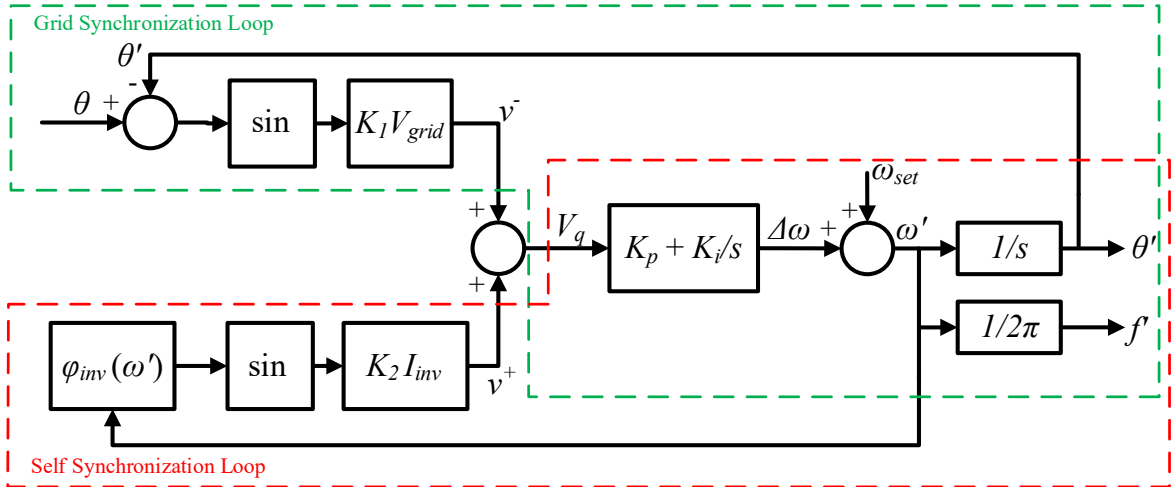


Figure 3.2: Quasi-static PLL model.

The parameters K_1 and K_2 can be expressed as [141]:

$$K_1 = \frac{z_L(\omega)}{z_L(\omega) + z_g(\omega)} \quad (9)$$

$$K_2 = \frac{z_L(\omega')z_g(\omega')}{z_L(\omega') + z_g(\omega')} \quad (10)$$

where ω is the grid frequency and $z_L(\omega)$ and $z_g(\omega)$ are the local load equivalent impedance and the grid impedance both at the grid frequency, respectively.

As soon as islanding occurs, due to loss of grid synchronization, the PLL goes through self synchronization. The self synchronization loop tends to drive θ' away from the PCC phase angle θ . From (8), it can be concluded that in a stiff grid-connected system ($z_g = 0$), $\varphi_{inv}(\omega')$ becomes zero, and the self synchronization loop disappears.

In a practical grid-connected system, the grid synchronization loop adjusts the input error $\theta - \theta'$ such that v^- eliminates v^+ and V_q becomes zero. Upon islanding, the grid synchronization loop disappears and V_q steps from zero to v^+ . Based on (8) and (10), the value of v^+ after islanding ($z_g = \infty$) becomes:

$$v^+ = |z_L(\omega')| I_{inv} \sin(\angle z_L(\omega')) \quad (11)$$

Subsequently, the inverter voltage and frequency approach different values corresponding to a new equilibrium determined by power mismatches [143].

Considering the PLL behaviour, this thesis introduces a passive IDM that operates based on the variations of the V_q . The maximum post-islanding value of V_q can be determined using (11) for any system, based on the total equivalent load impedance and the maximum inverter current magnitude. Hence, an appropriate value for the V_q threshold can be systematically determined based on the information of the equivalent load and inverter. Figure 3.3 shows a flowchart of the proposed algorithm. A second-order lowpass Butterworth filter with a cut-off frequency of 100 Hz, and a 3 ms timer are utilized to prevent false detection of non-islanding surges or malfunction due to the presence of noise in the system. The 3 ms timer is chosen such that the adverse effect of high-frequency disturbances is mitigated without unnecessary prolongation of islanding detection.

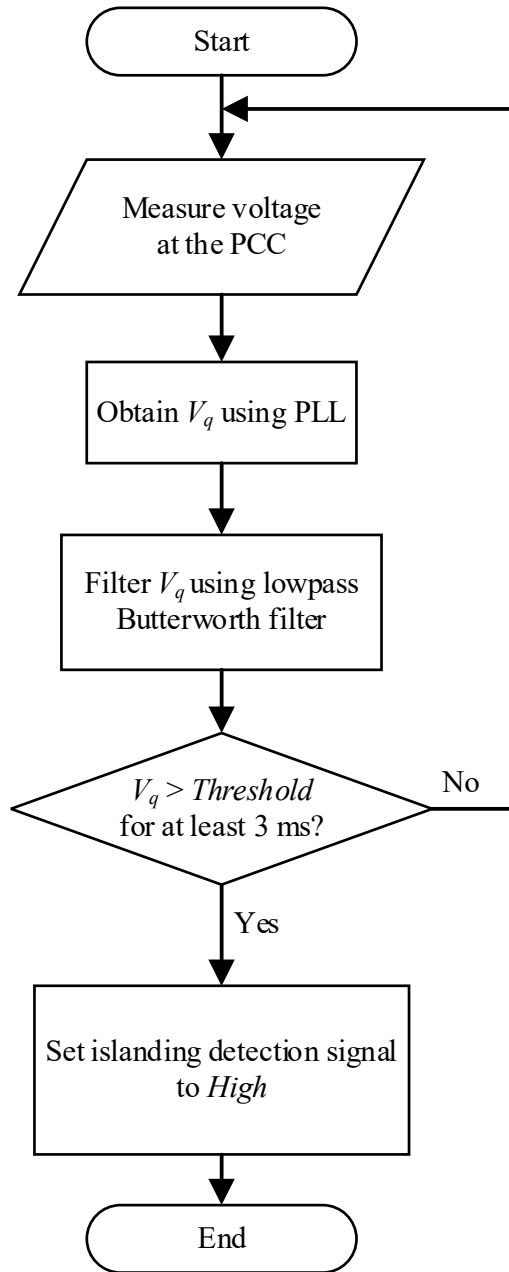


Figure 3.3: Flowchart of the proposed IDM.

Chapter 4

4 Performance Evaluation

This chapter investigates the performance of the proposed passive IDM under several operating conditions and compares it with those of the most commonly used passive IDMs through various islanding and non-islanding disturbances. The studies include time-domain simulations in the PSCAD/EMTDC software environment and experimental tests conducted using the hybrid microgrid test platform of Figure 1.4.

The operating quantities obtained from measurements conducted on the hybrid microgrid test platform are post-processed in Matlab.

4.1 Islanding

The performance of the passive IDMs under an islanding event is investigated and compared through simulation studies conducted on the study system 1, and experimental tests using the study system 3.

For both simulation and hardware implementation of the investigated methods, the thresholds are chosen such that a compromise is made between islanding detection speed and reliability. An exception is UOV- and UOF-based IDMs, for which it is widely practiced to adapt the thresholds to the voltage and frequency requirements of IEEE 1547¹.

Figure 4.1 shows the variations of different operating quantities utilized for passive islanding detection under an islanding event in study system 1, at $t = 0.2$ s.

The experimental results representing the variations of different operating quantities under an islanding event in study system 3, at $t = 0.2$ s, are presented in Figure 4.2.

¹ Refer to Table 1.

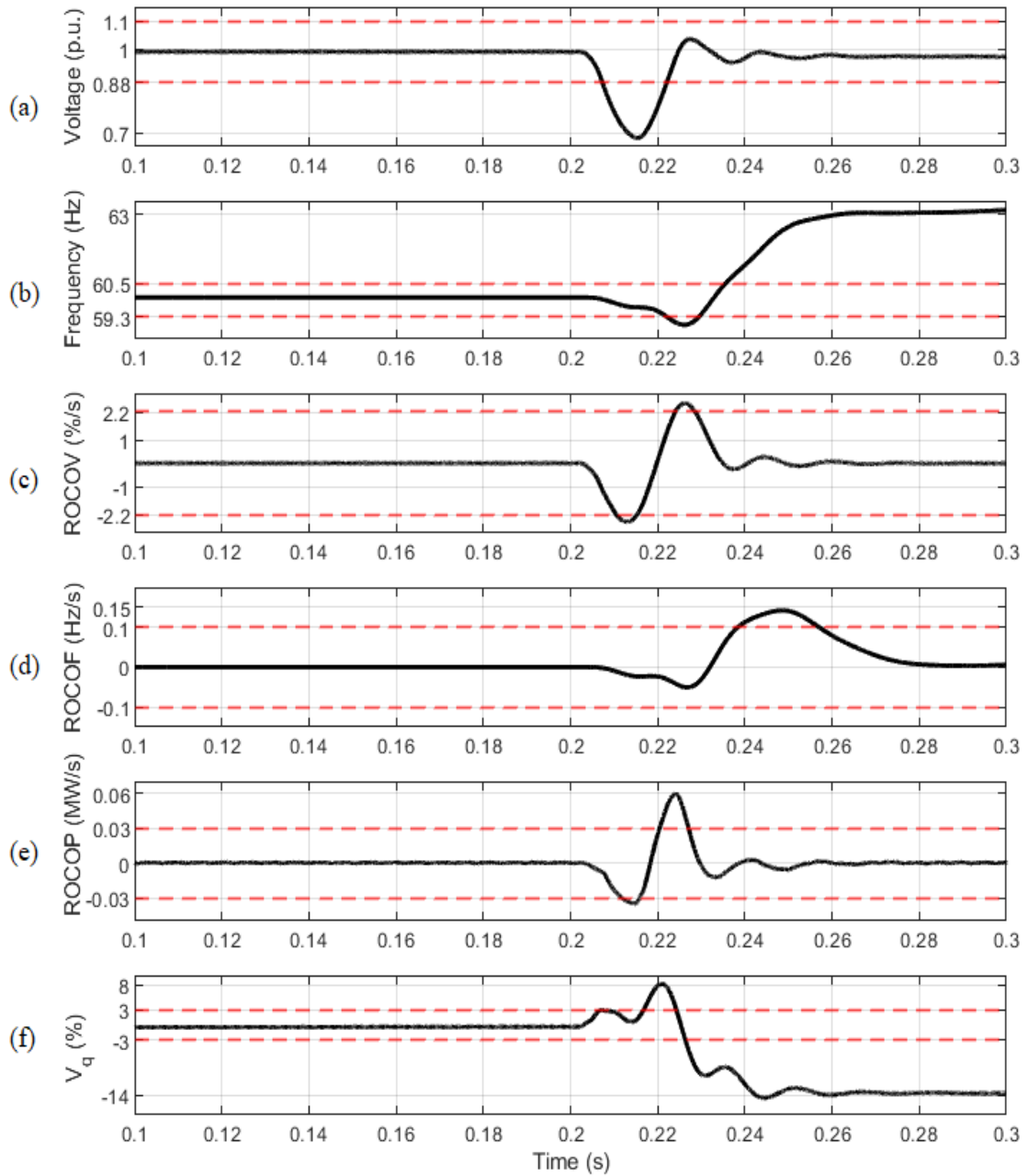


Figure 4.1: Variations of different operating quantities utilized for passive islanding detection under an islanding event in the study system 1, at $t = 0.2$ s (simulation results): (a) PCC voltage magnitude, (b) frequency, (c) ROCOV, (d) ROCOF, (e) ROCOP, and (f) q-axis voltage V_q .

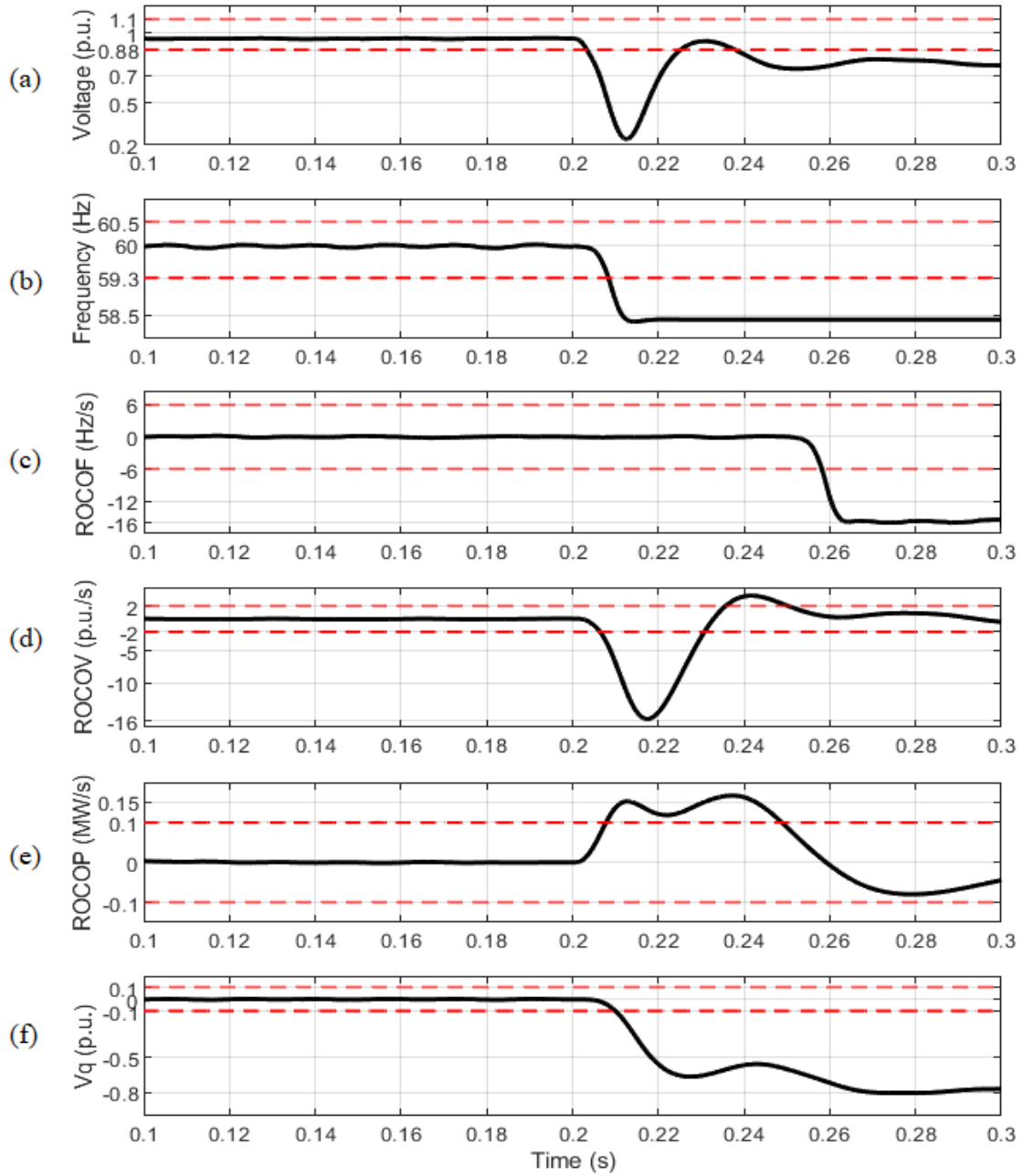


Figure 4.2: Variations of different operating quantities utilized for passive islanding detection under islanding event in the study system 3, at $t = 0.2$ s (experimental results): (a) PCC voltage magnitude, (b) frequency, (c) ROCOF, (d) ROCOV, (e) ROCOP, and (f) q-axis voltage V_q .

4.1.1 Non-Detection Zone

The study system 2 is utilized to evaluate the NDZ of the IDMs. The equivalent parallel RLC load¹ is calculated according to the requirements of IEEE 1547 for the worst scenario, i.e., zero power mismatch between the DER output and load, as well as $\pm 5\%$, $\pm 10\%$, and $\pm 15\%$ mismatch in both active and reactive powers. A positive mismatch indicates power surplus and a negative mismatch indicates power deficit. The load quality factor Q_f is assumed to be equal to 1, as recommended by the IEEE 1547 standard.

Figure 4.3 shows the variations of the operating parameters under an islanding event in the study system 2 at $t = 0.2$ s, considering a -15% active and reactive power mismatch. The ROCOV-, ROCOF-, and ROCOP-based IDMs fail to detect the islanding event.

Figure 4.4 compares the IDMs considering a $+15\%$ power mismatch. In this case, only the UOF-based and the proposed IDM detect the islanding event. Also, the ROCOF-based IDM comes very close to the threshold which confirms that ROCOF-based islanding detection may lead to an NDZ of about 15% [56], [81], [84], [85].

¹ Refer to 1.5.2 for the description.

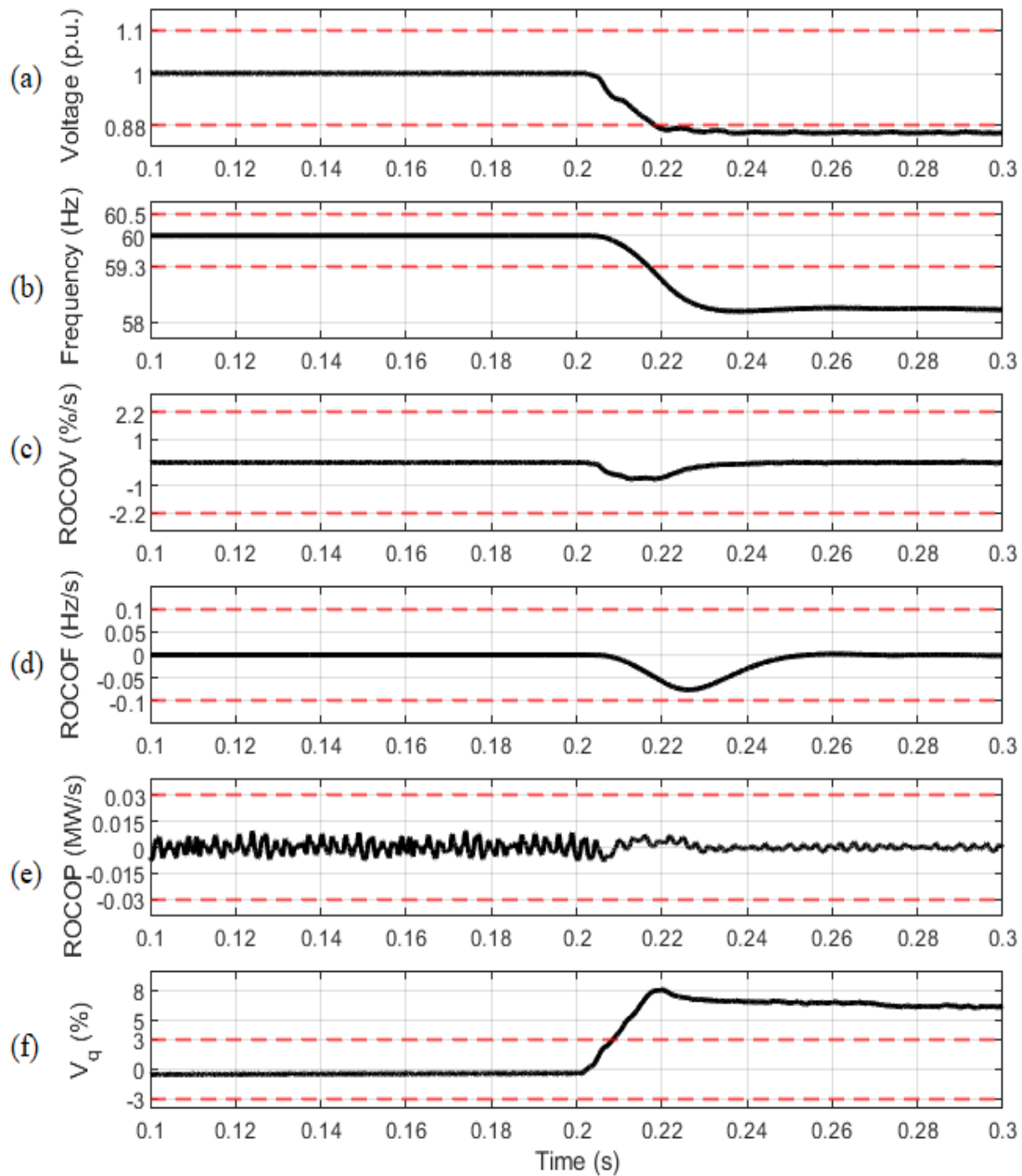


Figure 4.3: Variations of different operating quantities utilized for passive islanding detection under an islanding event in the study system 2, at $t = 0.2$ s, considering a -15% power mismatch (simulation results): (a) PCC voltage magnitude, (b) frequency, (c) ROCOV, (d) ROCOF, (e) ROCOP, and (f) q-axis voltage V_q .

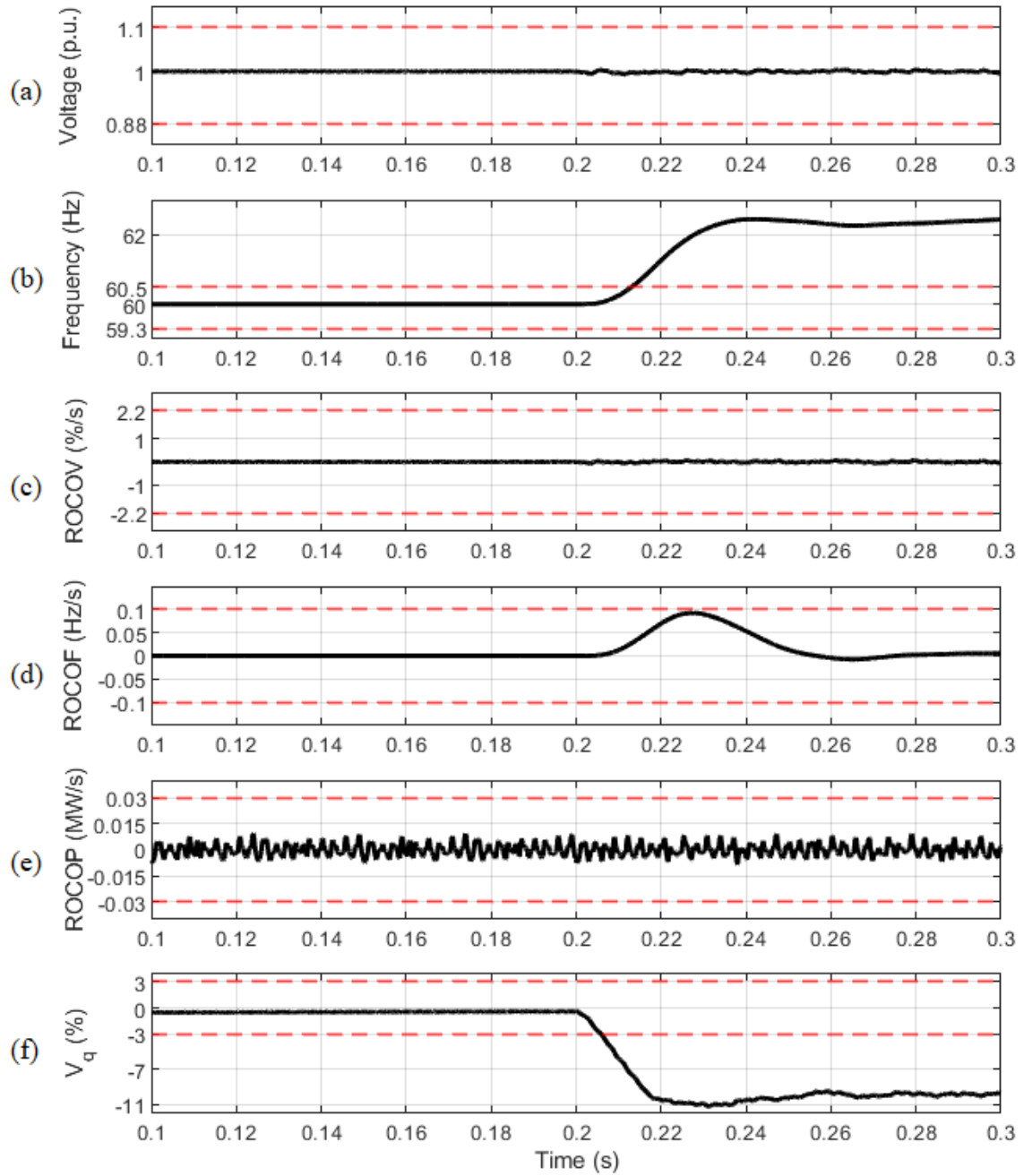


Figure 4.4: Variations of different operating quantities utilized for passive islanding detection under an islanding event in the study system 2, at $t = 0.2$ s, considering a +15% power mismatch (simulation results): (a) PCC voltage magnitude, (b) frequency, (c) ROCOV, (d) ROCOF, (e) ROCOP, and (f) q-axis voltage V_q .

Figure 4.5 shows the variations of the operating parameters under an islanding event in study system 2 at $t = 0.2$ s, considering a -10% active and reactive power mismatch. As shown in Figure 4.5 (b) and (f), the UOF-based method and the proposed IDM detect the islanding event. Figure 4.6 shows the zoomed-in variations of the voltage magnitude and the generated islanding detection signal (IDS). The voltage magnitude crosses the lower threshold for not a sufficiently long period to generate a pulse, meaning the UOV-based IDM fails to reliably detect islanding.

The variations of the operating parameters under an islanding event in the study system 2 at $t = 0.2$ s, considering a $+10\%$ active and reactive power mismatch, are provided in Figure 4.7. Figure 4.7 (b) and (f) illustrate that only the UOF-based and the proposed IDM can detect the islanding event.

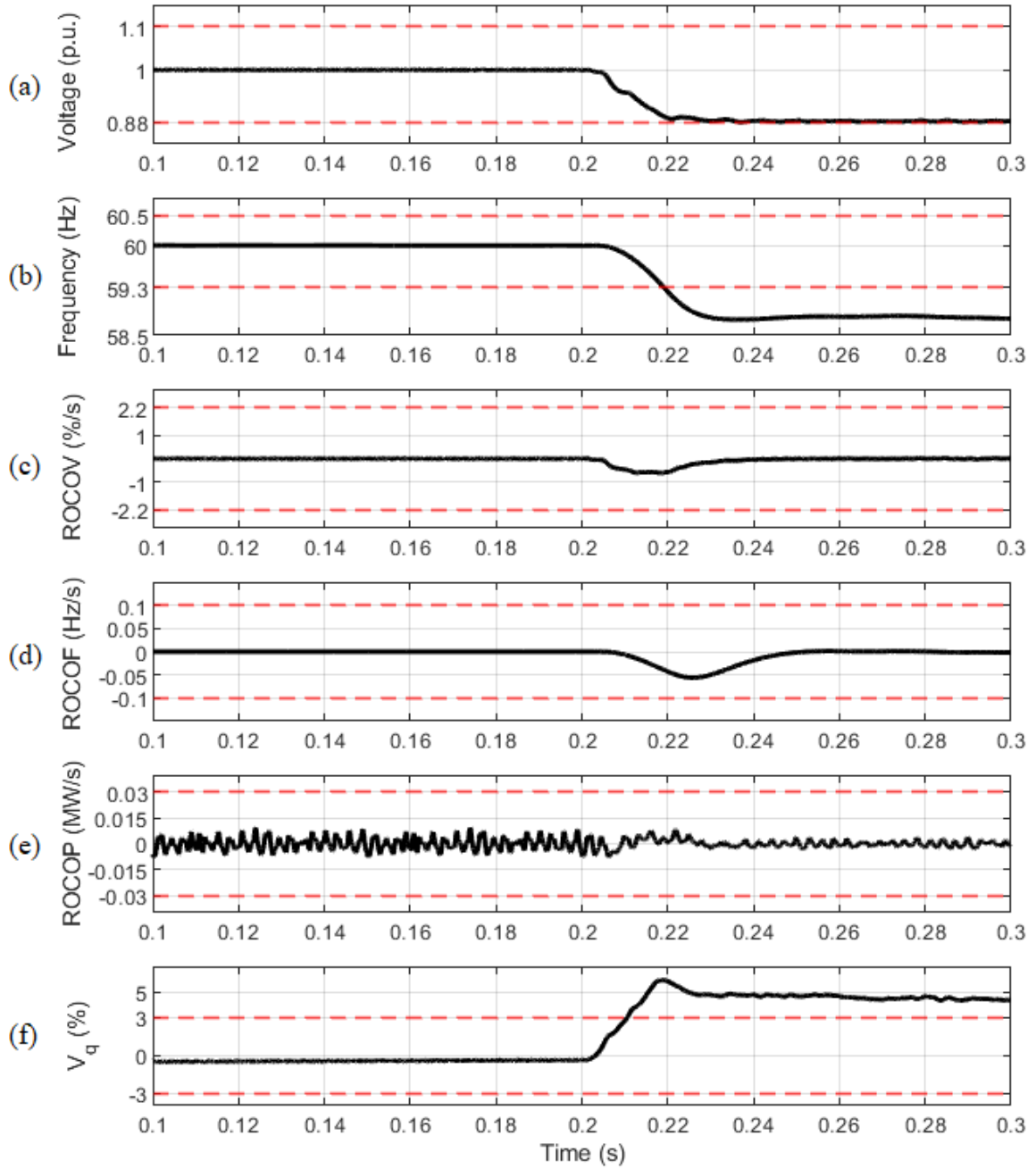


Figure 4.5: Variations of different operating quantities utilized for passive islanding detection under an islanding event in the study system 2, at $t = 0.2$ s, considering a -10% power mismatch (simulation results): (a) PCC voltage magnitude, (b) frequency, (c) ROCOV, (d) ROCOF, (e) ROCOP, and (f) q-axis voltage V_q .

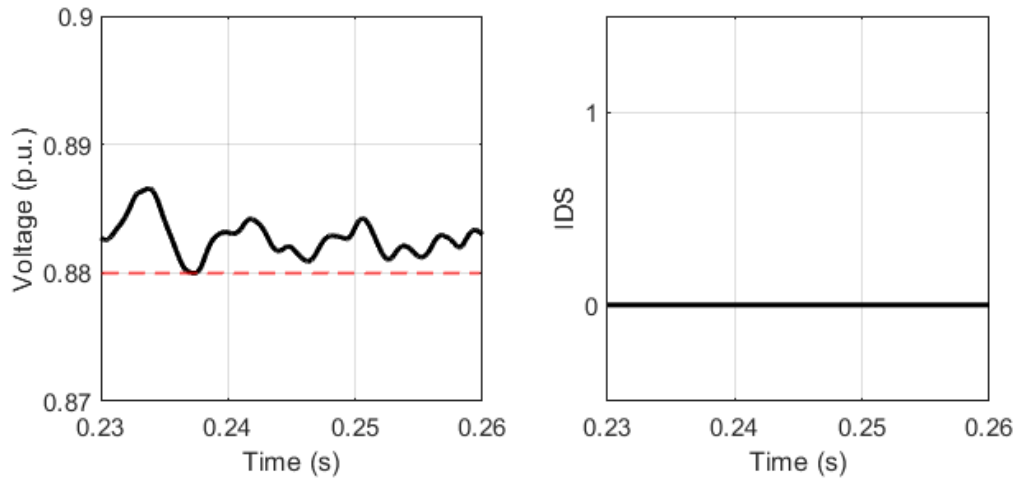


Figure 4.6: Variations of voltage magnitude under an islanding event considering a -10% power mismatch (left) and the generated IDS (right), zoomed-in version of Figure 4.5 (a).

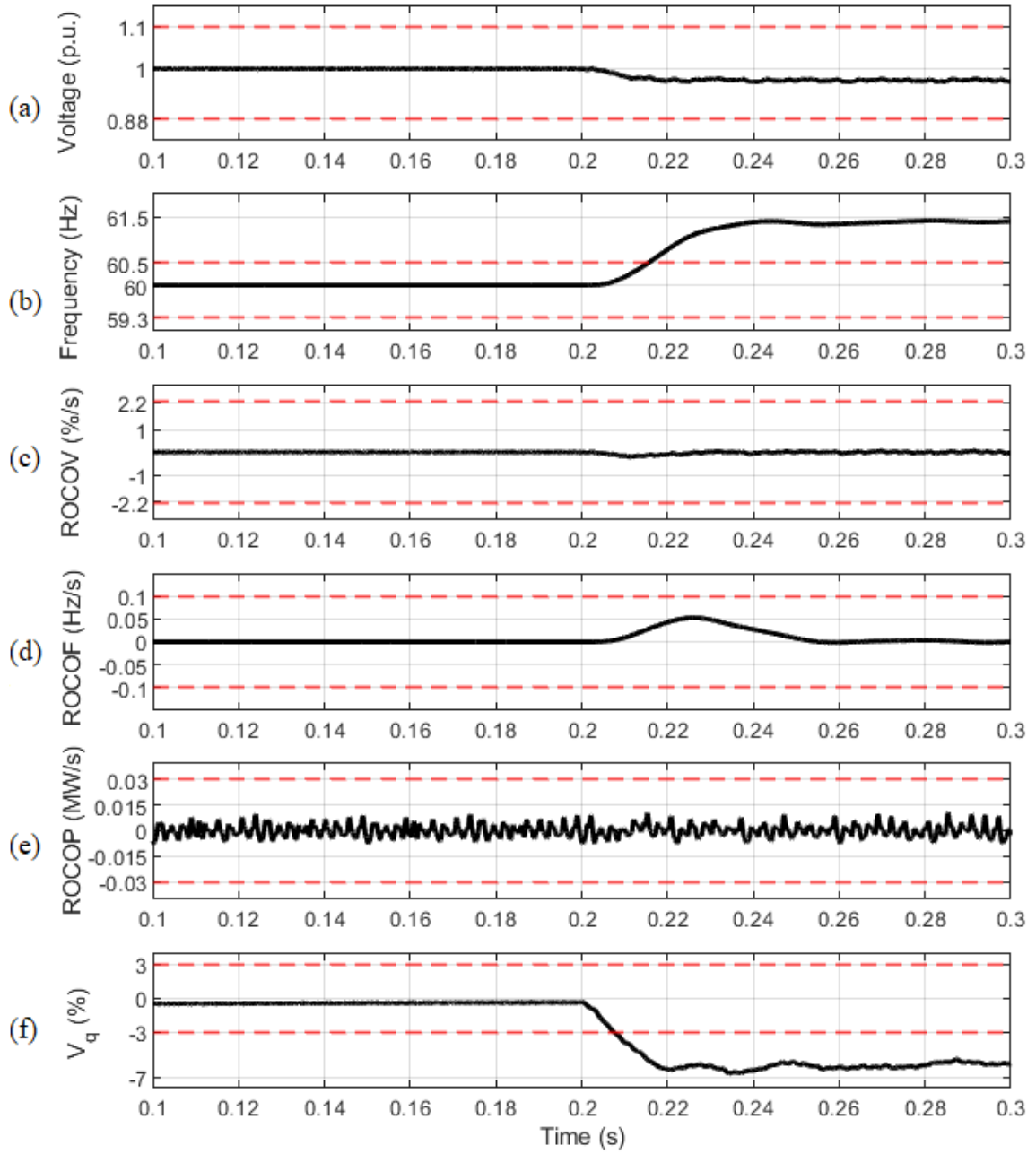


Figure 4.7: Variations of different operating quantities utilized for passive islanding detection under an islanding event in the study system 2, at $t = 0.2$ s, considering a +10% power mismatch (simulation results): (a) PCC voltage magnitude, (b) frequency, (c) ROCOV, (d) ROCOF, (e) ROCOP, and (f) q-axis voltage V_q .

Figure 4.8 illustrates the variations of the operating parameters under an islanding event in study system 2 at $t = 0.2$ s, considering -5% active and reactive power mismatch. Figure 4.8 (f) shows that the proposed IDM detects the islanding event. Figure 4.9 presents a closer look into the variations of the frequency, which indicates successful islanding detection.

Figure 4.10 shows the variations of the operating parameters under an islanding event in the study system 2 at $t = 0.2$ s, considering $+5\%$ active and reactive power mismatch. In this case, the UOF-based IDM can detect islanding as shown in Figure 4.10 (b). A zoomed-in version of Figure 4.10 (f) is provided in Figure 4.11, which shows that V_q exceeds the threshold for longer than the 3 ms delay. Therefore, the proposed IDM successfully detects the islanding event considering a $+5\%$ power mismatch.

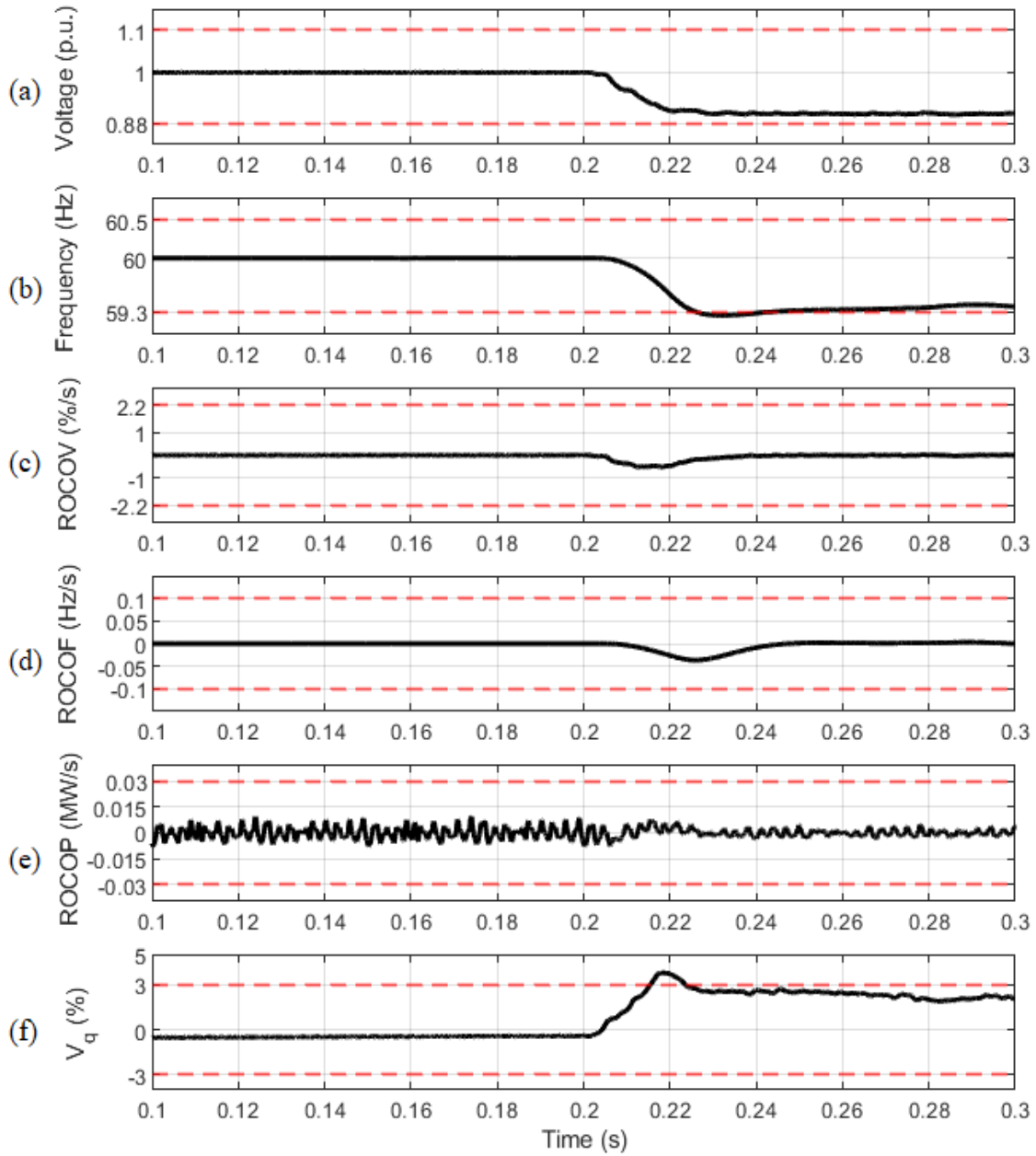


Figure 4.8: Variations of different operating quantities utilized for passive islanding detection under an islanding event in the study system 2, at $t = 0.2$ s, considering a -5% power mismatch (simulation results): (a) PCC voltage magnitude, (b) frequency, (c) ROCOV, (d) ROCOF, (e) ROCOP, and (f) q-axis voltage V_q .

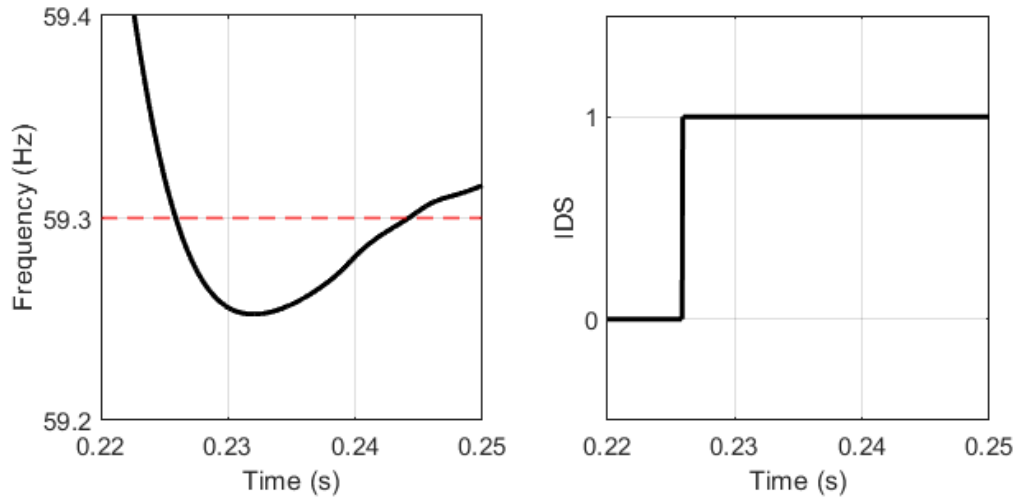


Figure 4.9: Variations of frequency under an islanding event considering a -5% power mismatch (left) and the generated IDS (right), zoomed-in version of Figure 4.8 (b).

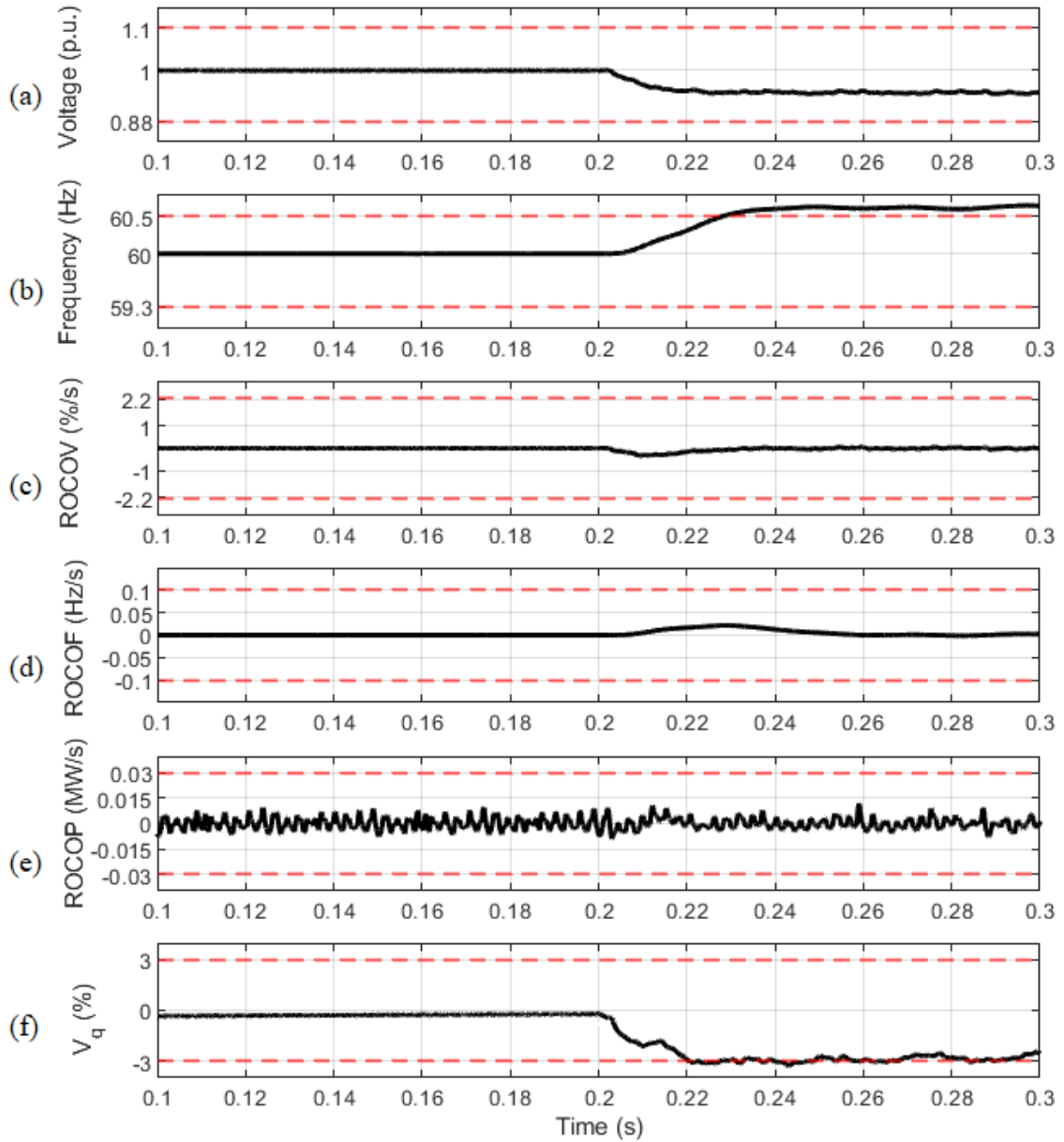


Figure 4.10: Variations of different operating quantities utilized for passive islanding detection under an islanding event in the study system 2, at $t = 0.2$ s, considering a +5% power mismatch (simulation results): (a) PCC voltage magnitude, (b) frequency, (c) ROCOV, (d) ROCOF, (e) ROCOP, and (f) q-axis voltage V_q .

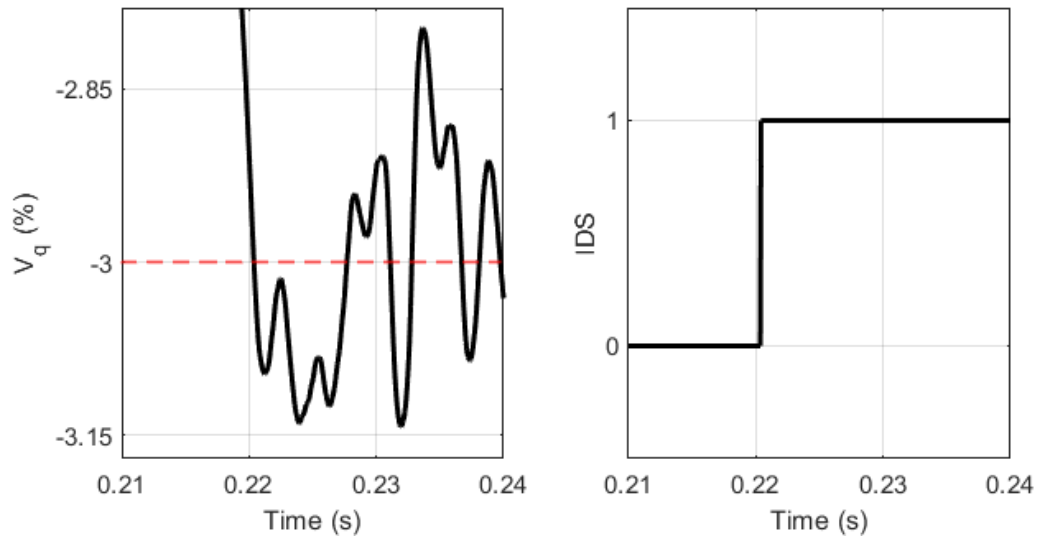


Figure 4.11: Variations of q-axis voltage V_q under an islanding event considering a +5% power mismatch (left) and the generated IDS (right), zoomed-in version of Figure 4.10 (f).

Finally, Figure 4.12 compares the performance of the investigated IDMs for 0% active and reactive power mismatches. As expected, none of the IDMs can detect the occurrence of islanding in this case due to the inherent limitation of all passive IDMs.

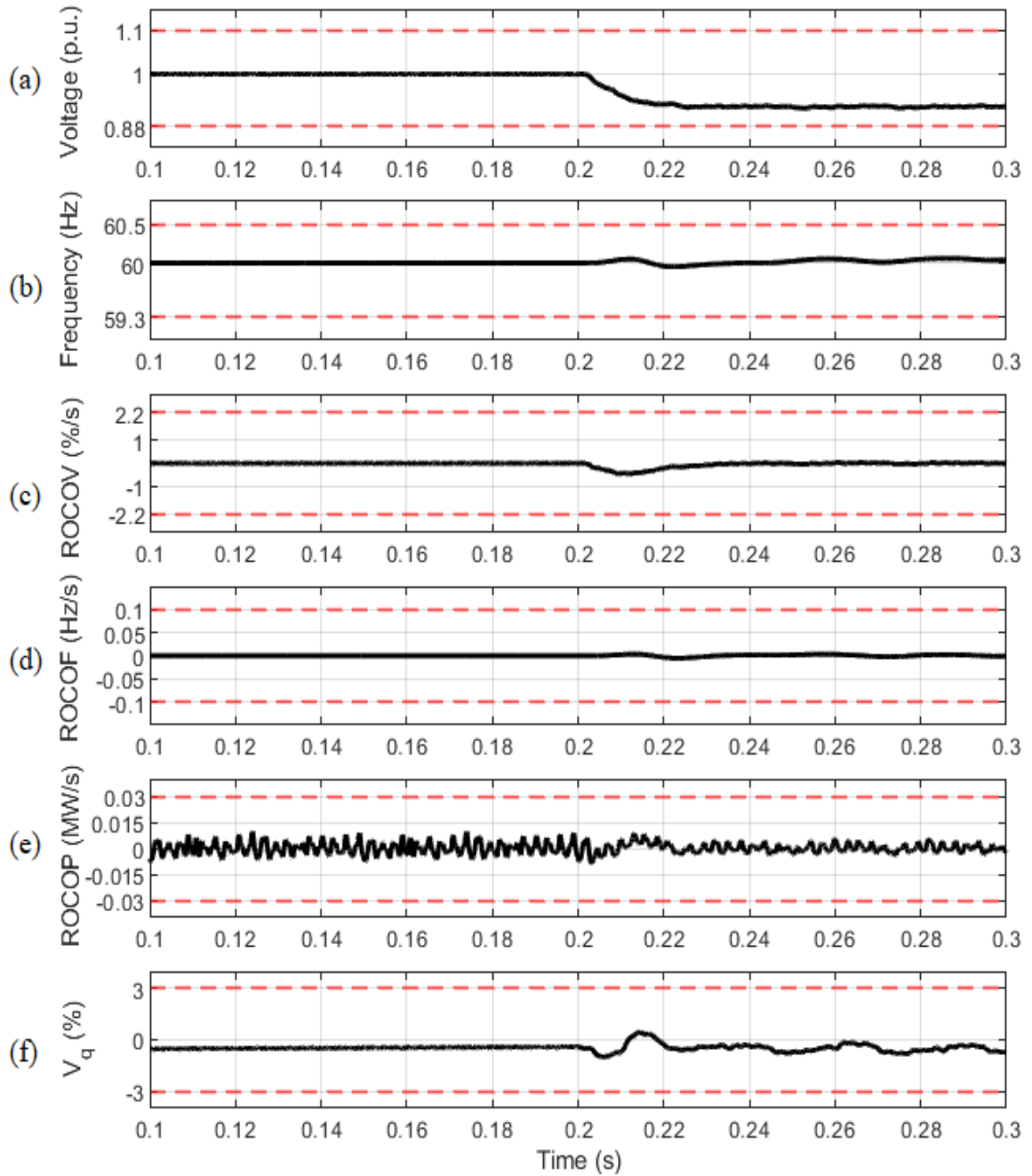


Figure 4.12: Variations of different operating quantities utilized for passive islanding detection under an islanding event in the study system 2, at $t = 0.2$ s, considering a 0% power mismatch (simulation results): (a) PCC voltage magnitude, (b) frequency, (c) ROCOV, (d) ROCOF, (e) ROCOP, and (f) q-axis voltage V_q .

Table 3 summarizes the simulation results obtained from NDZ studies conducted on the study system 2 under different power mismatch scenarios. The UOF-based and the proposed method operate reliably under power mismatches as small as $\pm 5\%$. However, none of them can detect islanding in case of perfect power balance. It should be noted that in practice, there is always some power mismatch between the DER output and the load [48].

Table 3: NDZ of the Investigated IDMs.

Power Mismatch (%)	Performance					
	UOV	UOF	ROCOV	ROCOF	ROCOP	Proposed IDM
+15	Failed	✓	Failed	Failed	Failed	✓
+10	Failed	✓	Failed	Failed	Failed	✓
+5	Failed	✓	Failed	Failed	Failed	✓
0	Failed	Failed	Failed	Failed	Failed	Failed
-5	Failed	✓	Failed	Failed	Failed	✓
-10	Failed	✓	Failed	Failed	Failed	✓
-15	✓	✓	Failed	Failed	Failed	✓

4.1.2 Detection Time

Table 4 presents the detection time of each IDM based on the results of the islanding studies conducted on the study system 1, study system 2, and study system 3.

Table 4: Detection Time of the Investigated IDMs.

	Detection Time (ms)			Average Detection Time
	Simulation		Experimental	
	Study System 1 ¹	Study System 2 (30% power deficit)	Study System 3 ²	
UOV	7	9	4	within one cycle
UOF	22	13	9	within one cycle
ROCOV	11	10	7	within one cycle
ROCOF	38	18	58	within three cycles
ROCOP	22	11	8	within one cycle
Proposed IDM	22	7	24	within two cycles

¹ Refer to Appendix A for the load specifications.

² Refer to Appendix B for the load specifications.

As shown in Table 4, the UOV- and ROCOV-based IDMs with detection times of less than one cycle, are the fastest among the investigated IDMs, and ROCOF with a detection time of around three cycles is the slowest method. The detection time of the proposed IDM is less than 2 cycles.

As per IEEE 1547-2018, a DER is required to detect islanding, discontinue to energize the system, and trip within 2 s of the formation of an island. Of course, this requirement is not strict and a faster islanding detection is desirable. The detection time of the proposed IDM is well below the requirements of IEEE 1547.

4.2 Non-Islanding Disturbances

4.2.1 Fault ‘F1’

In this case study, a single-phase-to-ground fault ‘F1’ (Figure 1.2), with a fault resistance $R_f = 0.01 \Omega$ occurs in the study system 1 at $t = 0.2$ s. Figure 4.13 shows the variations of different operating quantities utilized for passive islanding detection.

As shown in Figure 4.13 (a), the UOV-based IDM misidentifies fault ‘F1’ as islanding. Figure 4.14 represents a zoomed-in version of Figure 4.13 (b) and the generated IDS, which indicates that the UOF-based IDM also detects ‘F1’ as islanding.

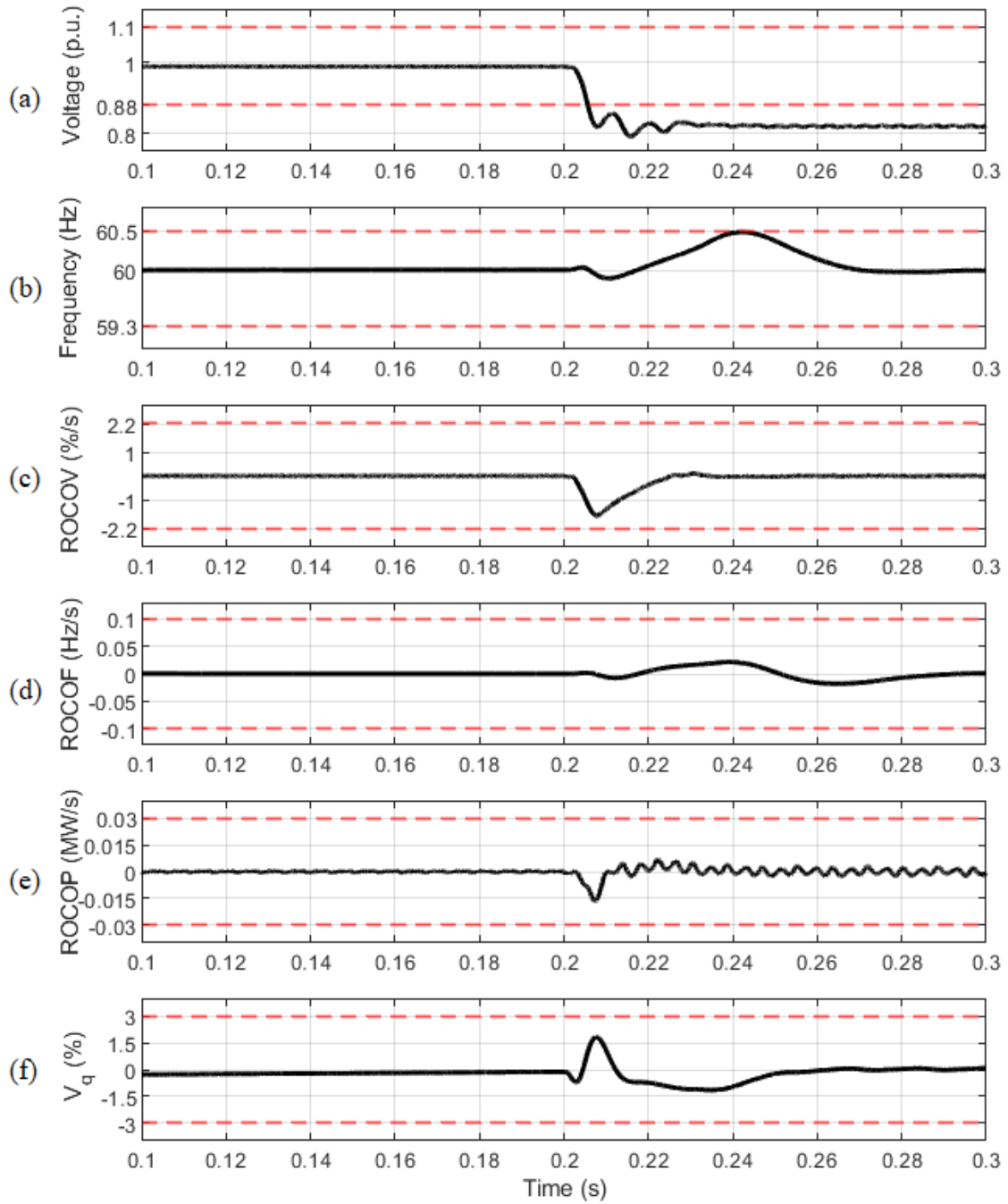


Figure 4.13: Variations of different operating quantities utilized for passive islanding detection under fault 'F1' in the study system 1, at $t = 0.2$ s (simulation results): (a) PCC voltage magnitude, (b) frequency, (c) ROCOV, (d) ROCOF, (e) ROCOP, and (f) q-axis voltage V_q .

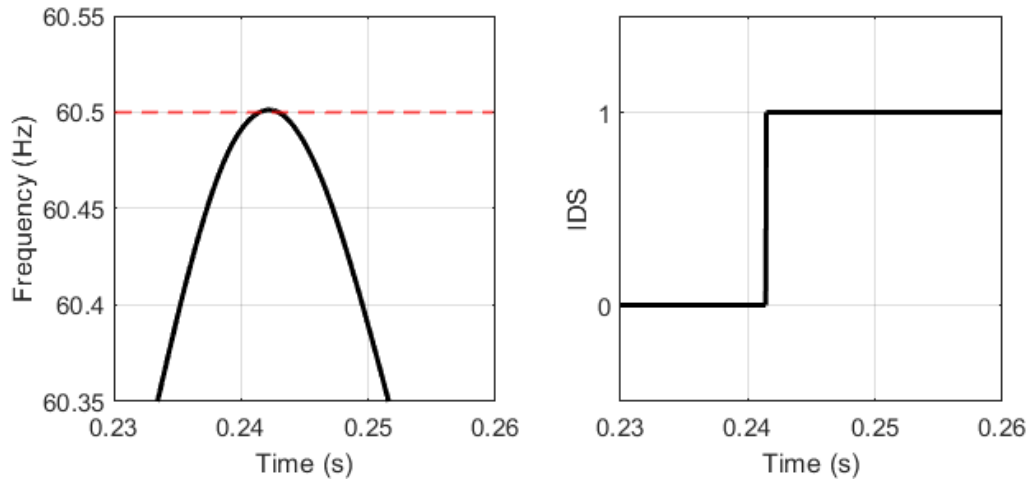


Figure 4.14: Variations of frequency under fault ‘F1’ (left) and the generated IDS (right), zoomed-in version of Figure 4.13 (b).

4.2.2 Fault ‘F2’

In this case study, a single-phase-to-ground fault ‘F2’ (as shown in Figure 1.2), with a fault resistance $R_f = 0.01 \Omega$ occurs in the study system 1 at $t = 0.2$ s. Figure 4.15 shows the variations of different operating quantities utilized for passive islanding detection.

Figure 4.15 (c) and (e) show that the ROCOV and ROCOP come very close to the thresholds, however, do not cause false detection. Figure 4.15 (a) shows that the UOV-based IDM detects ‘F2’ as islanding.

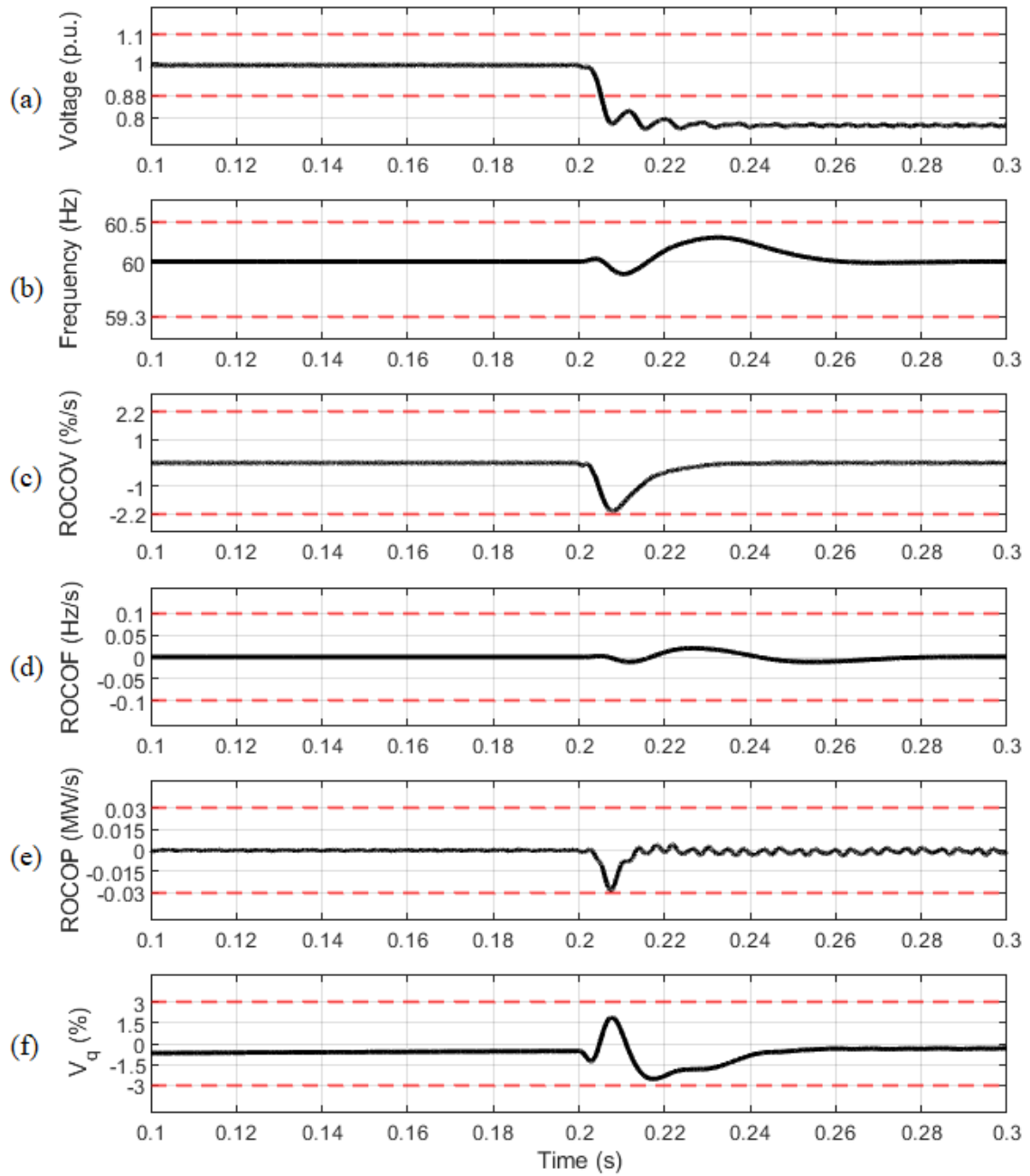


Figure 4.15: Variations of different operating quantities utilized for passive islanding detection under fault 'F2' in study system 1, at $t = 0.2$ s (simulation results): (a) PCC voltage magnitude, (b) frequency, (c) ROCOV, (d) ROCOF, (e) ROCOP, and (f) q-axis voltage V_q .

4.2.3 Motor Starting

In this case study, a 4.8 kV, 1.7 MVA motor (Figure 1.2) is started in the study system 1 at $t = 0.2$ s. Figure 4.16 shows the variations of different operating quantities utilized for passive islanding detection during motor starting. In this case, the voltage magnitude experiences the largest deviation, however, none of the IDMs misidentifies this disturbance.

The study system 3 is utilized to experimentally evaluate the performance of the IDMs under motor starting. A three-phase 15 W induction motor connected to bus 3 (Figure 1.4) is started at $t = 0.2$ s. Figure 4.17 (d) shows that the ROCOV-based IDM misidentifies this disturbance. As Figure 4.17 (a) illustrates, the UOV-based IDM comes very close to its lower threshold. However, as shown in Figure 4.18, it does not lead to nuisance detection.

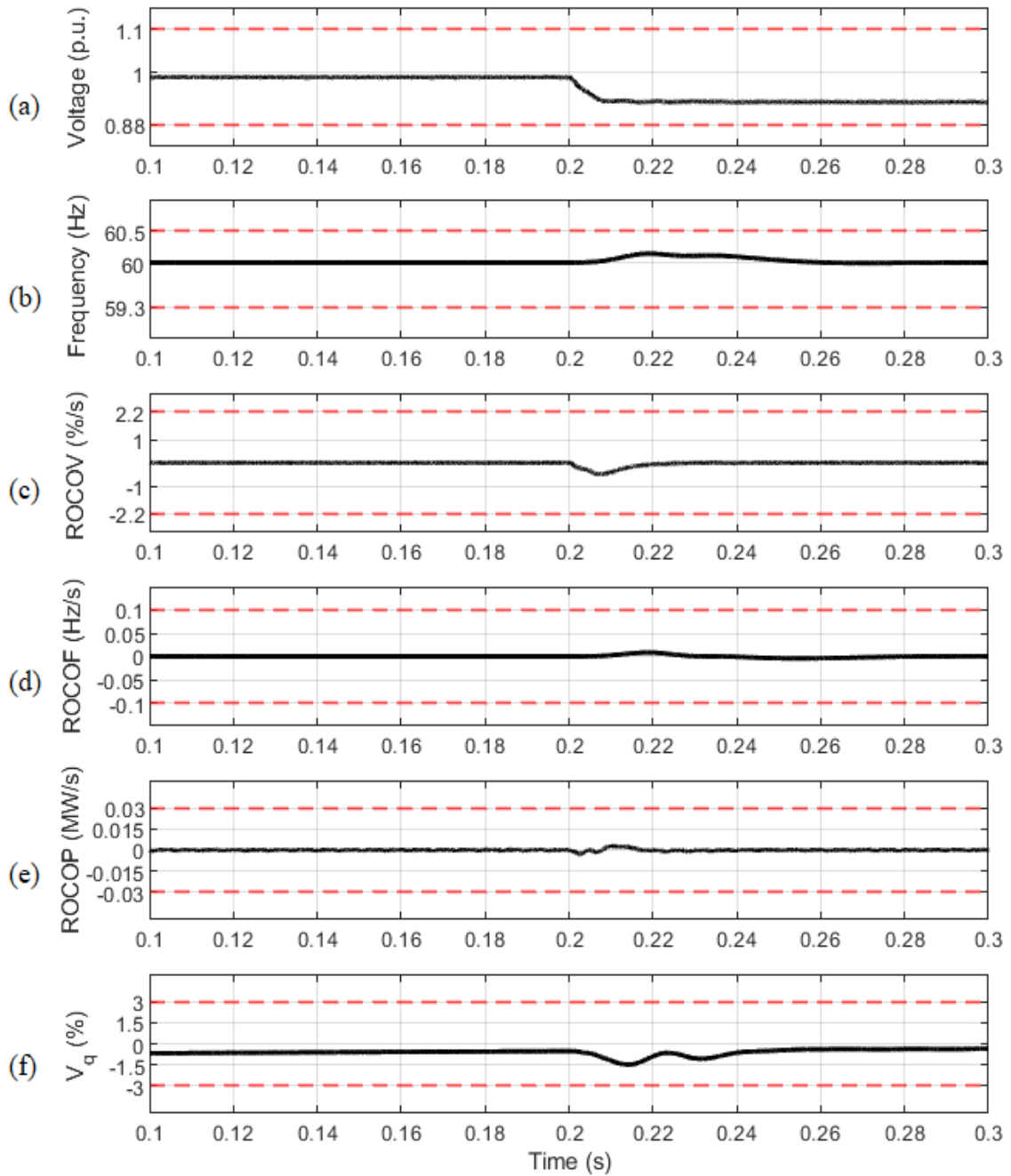


Figure 4.16: Variations of different operating quantities utilized for passive islanding detection under motor starting in the study system 1, at $t = 0.2$ s (simulation results): (a) PCC voltage magnitude, (b) frequency, (c) ROCOV, (d) ROCOF, (e) ROCOP, and (f) q-axis voltage V_q .

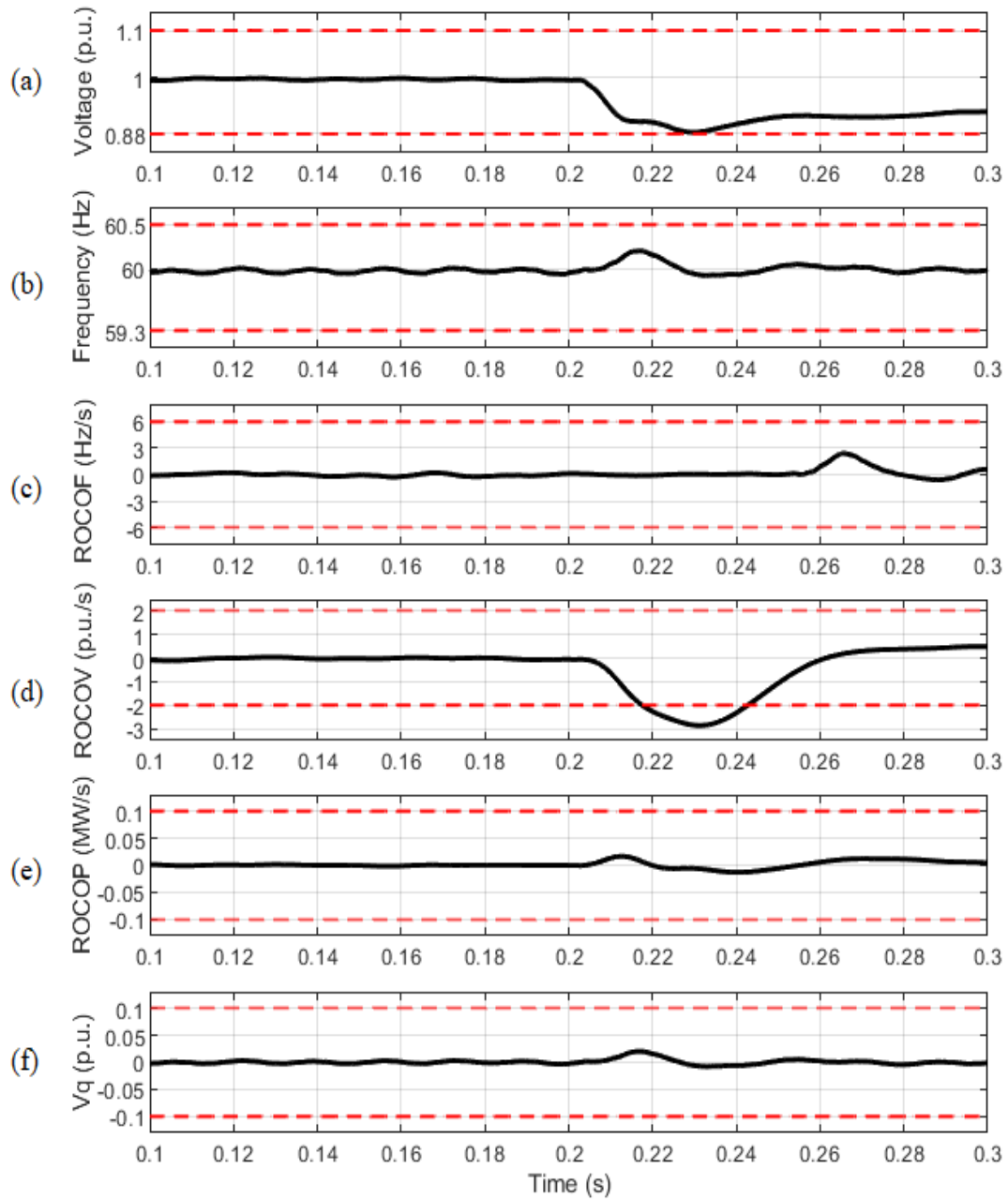


Figure 4.17: Variations of different operating quantities utilized for passive islanding detection under motor starting in the study system 3, at $t = 0.2$ s (experimental results): (a) PCC voltage magnitude, (b) frequency, (c) ROCOF, (d) ROCOV, (e) ROCOP, and (f) q-axis voltage V_q .

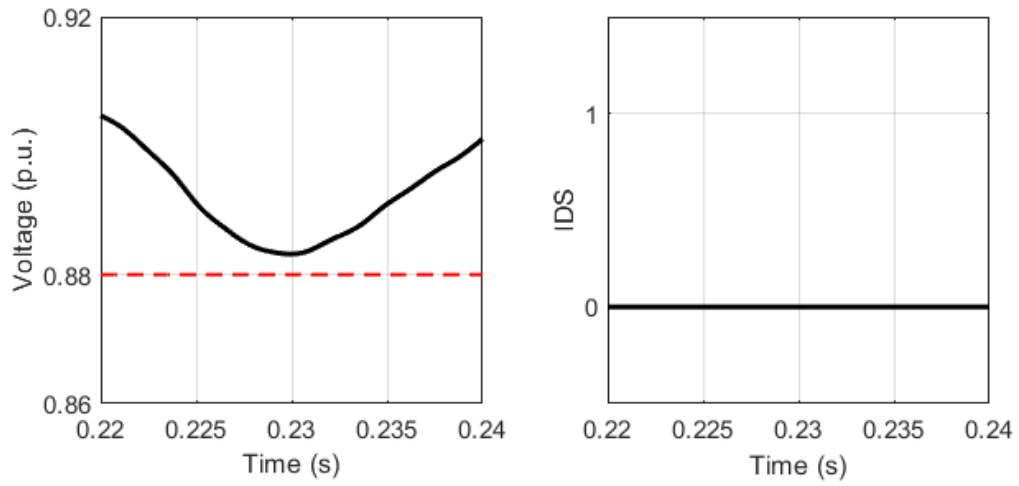


Figure 4.18: Variations of voltage magnitude under motor starting (left) and the generated IDS (right), zoomed-in version of Figure 4.17 (a).

4.2.4 Static Load Switching

In this case study, a 1000 kW, 1000 kVAR static load (load #16 in Figure 1.2) is switched on in the study system 1, at $t = 0.2$ s. The variations of the operating parameters under the event of load switching are illustrated in Figure 4.19, which does not show any false detection of the disturbance as islanding.

The study system 3 is utilized to experimentally evaluate the performance of the IDMs under the static load switching event. In this case, a 30 W AC load (AC-L3 in Figure 1.4) is switched on at $t = 0.2$ s. Figure 4.20 (d) shows that the ROCOV exceeds the lower threshold which indicates false detection of the disturbance as islanding. Even though the voltage magnitude does not exceed the threshold in Figure 4.20 (a), it is prone to nuisance detection.

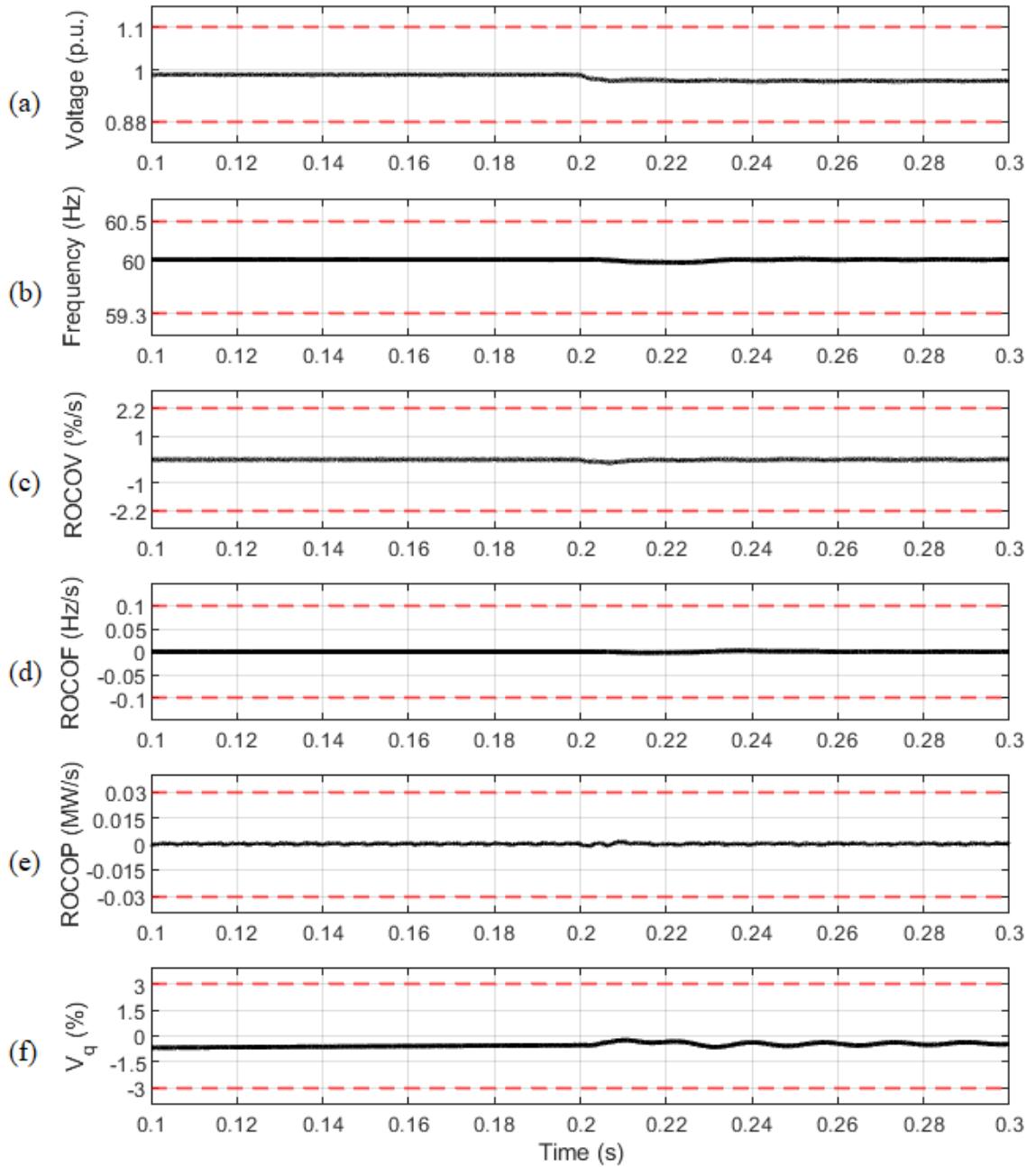


Figure 4.19: Variations of different operating quantities utilized for passive islanding detection under static load switching in the study system 1, at $t = 0.2$ s (simulation results): (a) PCC voltage magnitude, (b) frequency, (c) ROCOV, (d) ROCOF, (e) ROCOP, and (f) q-axis voltage V_q .

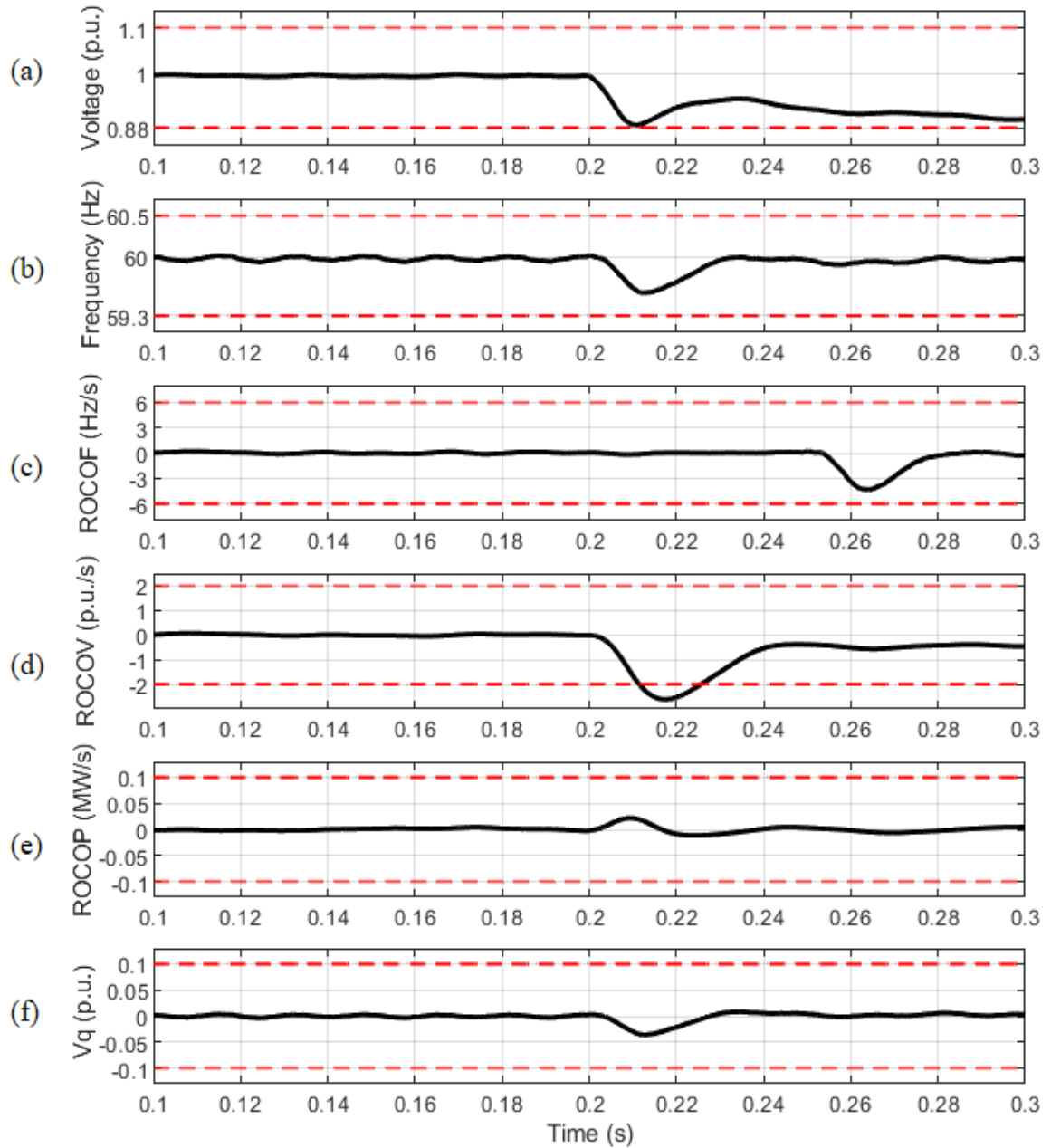


Figure 4.20: Variations of different operating quantities utilized for passive islanding detection under static load switching in the study system 3, at $t = 0.2$ s (experimental results): (a) PCC voltage magnitude, (b) frequency, (c) ROCOF, (d) ROCOV, (e) ROCOP, and (f) q-axis voltage V_q .

4.2.5 Nuisance Detection

The results of the non-islanding case studies from study systems 1 and 3 are compared and summarized in Table 5. As shown in the table, the ROCOF-based, ROCOP-based, and the proposed IDM do not cause false detection (FD), therefore, they show better security against the investigated non-islanding scenarios.

Table 5: Nuisance Detection in the Investigated IDMs.

	Study system 1 (Simulation Results)				Study system 3 (Experimental Results)	
	Fault F1	Fault F2	Motor starting	Static load switching	Motor starting	Static load switching
UOV	FD	FD	-	-	-	-
UOF	FD	-	-	-	-	-
ROCOV	-	-	-	-	FD	FD
ROCOF	-	-	-	-	-	-
ROCOP	-	-	-	-	-	-
Proposed IDM	-	-	-	-	-	-

Chapter 5

5 Conclusions

5.1 Conclusions

A novel passive IDM is introduced in this thesis. The proposed IDM utilizes an internal parameter of PLL, namely the q-axis component of voltage V_q , as an indicator of islanding. Upon islanding, V_q suddenly increases, and by applying an appropriate threshold, islanding can be detected quickly and reliably.

Similar to other passive IDMs, the proposed IDM does not degrade power quality or adversely affect the power system stability, as it does not require external signal injection. Also, it can be applied to multi-DER systems like study system 1 which comprises PV, WT and energy storage units. In addition, the proposed IDM is cost-effective; it does not require expensive hardware for communication and only utilizes the parameter obtained from an already-existing PLL.

The proposed method can detect islanding with an average time delay of 18 ms, which is well below the requirements of the IEEE 1547 standard. It

benefits from a small NDZ and can identify the islanding conditions in case of only $\pm 5\%$ power mismatch. Only the UOF-based IDM provides similar dependability, however, it shows low security against the investigated non-islanding events. The proposed IDM does not falsely detect non-islanding disturbances, and it provides the highest reliability among the investigated passive IDMs.

The competency of the proposed IDM is verified using multiple studies conducted on the realistic model of a Canadian rural distribution network as well as the IEEE recommended test system in the PSCAD software environment. Furthermore, the efficacy of the proposed IDM has been experimentally validated using a hybrid microgrid test platform.

5.2 Future Work

Although this study is focused on the detection of islanding using the variations of the q-axis component of voltage V_q , the effect of the PLL parameters on the proposed IDM can be investigated. The continuation of this study in the future includes analysis of the effect of PLL design on the performance of the proposed method.

The future work also includes investigating the performance of the proposed method using a wider range of study systems and the recorded signals of real-world islanding events.

References

- [1] R. Lasseter *et al.*, “Integration of distributed energy resources. The CERTS Microgrid Concept,” Apr. 2002, doi: 10.2172/799644.
- [2] M. F. Akorede, H. Hizam, and E. Pouresmaeil, “Distributed energy resources and benefits to the environment,” *Renewable and Sustainable Energy Reviews*, vol. 14, no. 2, pp. 724–734, Feb. 2010, doi: 10.1016/J.RSER.2009.10.025.
- [3] IEEE, “IEEE STD 1547-2018,” *IEEE Standard for Interconnection and Interoperability of Distributed Energy Resources with Associated Electric Power Systems Interfaces*, pp. 1–138, 2018.
- [4] M. Bakhshi, R. Noroozian, and G. B. Gharehpetian, “Novel islanding detection method for multiple DGs based on forced helmholtz oscillator,” *IEEE Transactions on Smart Grid*, vol. 9, no. 6, pp. 6448–6460, Nov. 2018, doi: 10.1109/TSG.2017.2712768.
- [5] H. H. Zeineldin and J. L. Kirtley, “Performance of the OVP/UVP and OFP/UFP method with voltage and frequency dependent loads,” *IEEE Transactions on Power Delivery*, vol. 24, no. 2, pp. 772–778, 2009, doi: 10.1109/TPWRD.2008.2002959.
- [6] S. C. Paiva, H. S. Sanca, F. B. Costa, and B. A. Souza, “Reviewing of anti-islanding protection,” *2014 11th IEEE/IAS International Conference on Industry Applications, IEEE INDUSCON 2014 - Electronic Proceedings*, Mar. 2014, doi: 10.1109/INDUSCON.2014.7059454.
- [7] F. Noor, R. Arumugam, and Y. Mohammad Vaziri, “Unintentional islanding and comparison of prevention techniques,” *Proceedings of the 37th Annual North American Power Symposium, 2005*, vol. 2005, pp. 90–96, 2005, doi: 10.1109/NAPS.2005.1560507.

- [8] A. Hussain, C. H. Kim, and A. Mehdi, "A Comprehensive Review of Intelligent Islanding Schemes and Feature Selection Techniques for Distributed Generation System," *IEEE Access*, vol. 9, pp. 146603–146624, 2021, doi: 10.1109/ACCESS.2021.3123382.
- [9] M. Elazzaoui, "An Effective Islanding Detection Method with Wavelet-Based Nuisance Tripping Suppressing," *IEEE Transactions on Power Electronics*, vol. 36, no. 12, pp. 13792–13801, Dec. 2021, doi: 10.1109/TPEL.2021.3087915.
- [10] F. Noor, R. Arumugam, and Y. Mohammad Vaziri, "Unintentional islanding and comparison of prevention techniques," *Proceedings of the 37th Annual North American Power Symposium, 2005*, vol. 2005, pp. 90–96, 2005, doi: 10.1109/NAPS.2005.1560507.
- [11] W. Teoh and C. Tan, "An overview of islanding detection methods in photovoltaic systems," *International Journal of Electrical and Computer Engineering*, vol. 5, no. 10, pp. 1341–1349, 2011, Accessed: Oct. 13, 2022. [Online]. Available: https://www.academia.edu/download/51080432/an-overview-of-islanding-detection-methods-in-photovoltaic-systems_-_Copy.pdf
- [12] R. Bakhshi-Jafarabadi, J. Sadeh, and M. Popov, "Maximum power point tracking injection method for islanding detection of grid-connected photovoltaic systems in microgrid," *IEEE Transactions on Power Delivery*, vol. 36, no. 1, pp. 168–179, Feb. 2021, doi: 10.1109/TPWRD.2020.2976739.
- [13] S. D. Kermany, M. Joorabian, S. Deilami, and M. A. S. Masoum, "Hybrid Islanding Detection in Microgrid with Multiple Connection Points to Smart Grids Using Fuzzy-Neural Network," *IEEE Transactions on Power Systems*, vol. 32, no. 4, pp. 2640–2651, Jul. 2017, doi: 10.1109/TPWRS.2016.2617344.
- [14] R. Bakhshi-Jafarabadi, J. Sadeh, J. de J. Chavez, and M. Popov, "Two-Level Islanding Detection Method for Grid-Connected Photovoltaic System-Based Microgrid with Small Non-Detection Zone," *IEEE Transactions on Smart Grid*, vol. 12, no. 2, pp. 1063–1072, Mar. 2021, doi: 10.1109/TSG.2020.3035126.

- [15] R. Bekhradian, M. Davarpanah, and M. Sanaye-Pasand, "Novel Approach for Secure Islanding Detection in Synchronous Generator Based Microgrids," *IEEE Transactions on Power Delivery*, vol. 34, no. 2, pp. 457–466, Apr. 2019, doi: 10.1109/TPWRD.2018.2869300.
- [16] T. Werho, V. Vittal, S. Kolluri, and S. M. Wong, "A potential island formation identification scheme supported by PMU measurements," *IEEE Transactions on Power Systems*, vol. 31, no. 1, pp. 423–431, Jan. 2016, doi: 10.1109/TPWRS.2015.2402130.
- [17] R. Sun and V. A. Centeno, "Wide area system islanding contingency detecting and warning scheme," *IEEE Transactions on Power Systems*, vol. 29, no. 6, pp. 2581–2589, Nov. 2014, doi: 10.1109/TPWRS.2014.2317802.
- [18] W. Wang, J. Kliber, and W. Xu, "A scalable power-line-signaling-based scheme for islanding detection of distributed generators," *2009 IEEE Power and Energy Society General Meeting, PES '09*, 2009, doi: 10.1109/PES.2009.5275794.
- [19] W. Wang, J. Kliber, G. Zhang, W. Xu, B. Howell, and T. Palladino, "A power line signaling based scheme for anti-islanding protection of distributed generators - Part II: Field test results," *IEEE Transactions on Power Delivery*, vol. 22, no. 3, pp. 1767–1772, 2007, doi: 10.1109/TPWRD.2007.899620.
- [20] W. Xu, G. Zhang, C. Li, W. Wang, G. Wang, and J. Kliber, "A power line signaling based technique for anti-islanding protection of distributed generators - Part I: Scheme and analysis," *IEEE Transactions on Power Delivery*, vol. 22, no. 3, pp. 1758–1766, 2007, doi: 10.1109/TPWRD.2007.899618.
- [21] Y. M. Makwana and B. R. Bhalja, "Experimental Performance of an Islanding Detection Scheme Based on Modal Components," *IEEE Transactions on Smart Grid*, vol. 10, no. 1, pp. 1025–1035, Jan. 2019, doi: 10.1109/TSG.2017.2757599.

- [22] H. H. Zeineldin, "A Q-f droop curve for facilitating islanding detection of inverter-based distributed generation," *IEEE Transactions on Power Electronics*, vol. 24, no. 3, pp. 665–673, 2009, doi: 10.1109/TPEL.2008.2008649.
- [23] P. Mahat, Z. Chen, B. Bak-Jensen, and C. L. Bak, "A simple adaptive overcurrent protection of distribution systems with distributed generation," *IEEE Transactions on Smart Grid*, vol. 2, no. 3, pp. 428–437, Sep. 2011, doi: 10.1109/TSG.2011.2149550.
- [24] B. Guha, R. J. Haddad, and Y. Kalaani, "Voltage Ripple-Based Passive Islanding Detection Technique for Grid-Connected Photovoltaic Inverters," *IEEE Power and Energy Technology Systems Journal*, vol. 3, no. 4, pp. 143–154, Jul. 2016, doi: 10.1109/JPETS.2016.2586847.
- [25] A. Samui and S. R. Samantaray, "Assessment of ROCPAD relay for islanding detection in distributed generation," *IEEE Transactions on Smart Grid*, vol. 2, no. 2, pp. 391–398, Jun. 2011, doi: 10.1109/TSG.2011.2125804.
- [26] H. Laaksonen, "Advanced islanding detection functionality for future electricity distribution networks," *IEEE Transactions on Power Delivery*, vol. 28, no. 4, pp. 2056–2064, 2013, doi: 10.1109/TPWRD.2013.2271317.
- [27] N. Liu, C. Diduch, L. Chang, and J. Su, "A Reference Impedance-Based Passive Islanding Detection Method for Inverter-Based Distributed Generation System," *IEEE Journal of Emerging and Selected Topics in Power Electronics*, vol. 3, no. 4, pp. 1205–1217, Dec. 2015, doi: 10.1109/JESTPE.2015.2457671.
- [28] A. Pouryekta, V. K. Ramachandaramurthy, N. Mithulananthan, and A. Arulampalam, "Islanding Detection and Enhancement of Microgrid Performance," *IEEE Systems Journal*, vol. 12, no. 4, pp. 3131–3141, Dec. 2018, doi: 10.1109/JSYST.2017.2705738.
- [29] V. R. Reddy and E. S. Sreeraj, "A Feedback-Based Passive Islanding Detection Technique for One-Cycle-Controlled Single-Phase Inverter Used in Photovoltaic

Systems,” *IEEE Transactions on Industrial Electronics*, vol. 67, no. 8, pp. 6541–6549, Aug. 2020, doi: 10.1109/TIE.2019.2938464.

- [30] A. Y. Hatata, E.-H. Abd-Raboh, and B. E. Sedhom, “A review of anti-islanding protection methods for renewable distributed generation systems,” *Journal of Electrical Engineering*, vol. 16, no. 1, p. 12, 2016.
- [31] S. R. Mohanty, N. Kishor, P. K. Ray, and J. Catalao, “Comparative study of advanced signal processing techniques for islanding detection in a hybrid distributed generation system,” in *2015 IEEE Power & Energy Society General Meeting*, Jul. 2015, pp. 1–1. doi: 10.1109/PESGM.2015.7285854.
- [32] P. K. Ray, N. Kishor, and S. R. Mohanty, “Islanding and power quality disturbance detection in grid-connected hybrid power system using wavelet and S-transform,” *IEEE Transactions on Smart Grid*, vol. 3, no. 3, pp. 1082–1094, 2012, doi: 10.1109/TSG.2012.2197642.
- [33] A. Samui and S. R. Samantaray, “Wavelet singular entropy-based islanding detection in distributed generation,” *IEEE Transactions on Power Delivery*, vol. 28, no. 1, pp. 411–418, 2013, doi: 10.1109/TPWRD.2012.2220987.
- [34] N. W. A. Lidula and A. D. Rajapakse, “A pattern-recognition approach for detecting power islands using transient signals-part II: Performance evaluation,” *IEEE Transactions on Power Delivery*, vol. 27, no. 3, pp. 1071–1080, 2012, doi: 10.1109/TPWRD.2012.2187344.
- [35] K. El-Arroudi, G. Joos, I. Kamwa, and D. T. McGillis, “Intelligent-based approach to islanding detection in distributed generation,” *IEEE Transactions on Power Delivery*, vol. 22, no. 2, pp. 828–835, Apr. 2007, doi: 10.1109/TPWRD.2007.893592.
- [36] W. K. A. Najy, H. H. Zeineldin, A. H. K. Alaboudy, and W. L. Woon, “A bayesian passive islanding detection method for inverter-based distributed generation using

- ESPRIT,” *IEEE Transactions on Power Delivery*, vol. 26, no. 4, pp. 2687–2696, Oct. 2011, doi: 10.1109/TPWRD.2011.2159403.
- [37] K. Naraghypour, K. Ahmed, and C. Booth, “A Comprehensive Review of Islanding Detection Methods for Distribution Systems,” *9th International Conference on Renewable Energy Research and Applications, ICRERA 2020*, pp. 428–433, Sep. 2020, doi: 10.1109/ICRERA49962.2020.9242850.
- [38] Q. Cui, K. El-Arroudi, and G. Joos, “Islanding detection of hybrid distributed generation under reduced non-detection zone,” *IEEE Transactions on Smart Grid*, vol. 9, no. 5, pp. 5027–5037, Sep. 2018, doi: 10.1109/TSG.2017.2679101.
- [39] M. S. Kim, R. Haider, G. J. Cho, C. H. Kim, C. Y. Won, and J. S. Chai, “Comprehensive Review of Islanding Detection Methods for Distributed Generation Systems,” *Energies 2019, Vol. 12, Page 837*, vol. 12, no. 5, p. 837, Mar. 2019, doi: 10.3390/EN12050837.
- [40] J. Zhang, D. Xu, G. Shen, Y. Zhu, N. He, and J. Ma, “An improved islanding detection method for a grid-connected inverter with intermittent bilateral reactive power variation,” *IEEE Transactions on Power Electronics*, vol. 28, no. 1, pp. 268–278, 2013, doi: 10.1109/TPEL.2012.2196713.
- [41] W. Cai, B. Liu, S. Duan, and C. Zou, “An islanding detection method based on dual-frequency harmonic current injection under grid impedance unbalanced condition,” *IEEE Transactions on Industrial Informatics*, vol. 9, no. 2, pp. 1178–1187, May 2013, doi: 10.1109/TII.2012.2209669.
- [42] G. Hernández-González and R. Iravani, “Current injection for active islanding detection of electronically- interfaced distributed resources,” *IEEE Transactions on Power Delivery*, vol. 21, no. 3, pp. 1698–1705, Jul. 2006, doi: 10.1109/TPWRD.2006.876980.
- [43] S. Yuyama *et al.*, “A high speed frequency shift method as a protection for islanding phenomena of utility interactive PV systems,” *Solar Energy Materials*

and Solar Cells, vol. 35, no. C, pp. 477–486, Sep. 1994, doi: 10.1016/0927-0248(94)90176-7.

- [44] A. Yafaoui, B. Wu, and S. Kouro, “Improved active frequency drift anti-islanding detection method for grid connected photovoltaic systems,” *IEEE Transactions on Power Electronics*, vol. 27, no. 5, pp. 2367–2375, 2012, doi: 10.1109/TPEL.2011.2171997.
- [45] J. Ma, H. Zheng, J. Zhao, X. Chen, J. Zhai, and C. Zhang, “An Islanding Detection and Prevention Method Based on Path Query of Distribution Network Topology Graph,” *IEEE Transactions on Sustainable Energy*, vol. 13, no. 1, pp. 81–90, Jan. 2022, doi: 10.1109/TSTE.2021.3104463.
- [46] H. R. Baghaee, D. Mlakic, S. Nikolovski, and T. Dragicevic, “Support Vector Machine-Based Islanding and Grid Fault Detection in Active Distribution Networks,” *IEEE Journal of Emerging and Selected Topics in Power Electronics*, vol. 8, no. 3, pp. 2385–2403, Sep. 2020, doi: 10.1109/JESTPE.2019.2916621.
- [47] R. Haider, C. H. Kim, T. Ghanbari, and S. B. A. Bukhari, “Harmonic-signature-based islanding detection in grid-connected distributed generation systems using Kalman filter,” *IET Renewable Power Generation*, vol. 12, no. 15, pp. 1813–1822, Nov. 2018, doi: 10.1049/IET-RPG.2018.5381.
- [48] Z. Ye, A. Kolwalkar, Y. Zhang, P. Du, and R. Walling, “Evaluation of anti-islanding schemes based on nondetection zone concept,” *IEEE Transactions on Power Electronics*, vol. 19, no. 5, pp. 1171–1176, Sep. 2004, doi: 10.1109/TPEL.2004.833436.
- [49] G. Wang, “Design Consideration and Performance Analysis of a Hybrid Islanding Detection Method Combining Voltage Unbalance/Total Harmonic Distortion and Bilateral Reactive Power Variation,” *CPSS Transactions on Power Electronics and Applications*, vol. 5, no. 1, pp. 86–100, Mar. 2020, doi: 10.24295/CPSSTPEA.2020.00008.

- [50] M. Seyedi, S. A. Taher, B. Ganji, and J. Guerrero, "A Hybrid Islanding Detection Method Based on the Rates of Changes in Voltage and Active Power for the Multi-Inverter Systems," *IEEE Transactions on Smart Grid*, vol. 12, no. 4, pp. 2800–2811, Jul. 2021, doi: 10.1109/TSG.2021.3061567.
- [51] D. Mlakic, H. R. Baghaee, and S. Nikolovski, "Gibbs Phenomenon-based Hybrid Islanding Detection Strategy for VSC-based Microgrids using Frequency Shift, THDU and RMSU," *IEEE Transactions on Smart Grid*, Sep. 2018, doi: 10.1109/TSG.2018.2883595.
- [52] X. Chen, Y. Li, and P. Crossley, "A novel hybrid islanding detection method for grid-connected microgrids with multiple inverter-based distributed generators based on adaptive reactive power disturbance and passive criteria," *IEEE Transactions on Power Electronics*, vol. 34, no. 9, pp. 9342–9356, Sep. 2019, doi: 10.1109/TPEL.2018.2886930.
- [53] B. Yu, M. Matsui, and G. Yu, "A review of current anti-islanding methods for photovoltaic power system," *Solar Energy*, vol. 84, no. 5, pp. 745–754, May 2010, doi: 10.1016/J.SOLENER.2010.01.018.
- [54] K. Naraghypour, I. Abdelsalam, K. H. Ahmed, and C. D. Booth, "Modified Q-f Droop Curve Method for Islanding Detection with Zero Non-Detection Zone," *IEEE Access*, vol. 9, pp. 158027–158040, 2021, doi: 10.1109/ACCESS.2021.3130370.
- [55] A. I. M. Isa, H. Mohamad, and Z. M. Yasin, "Evaluation on non-detection zone of passive islanding detection techniques for synchronous distributed generation," *ISCAIE 2015 - 2015 IEEE Symposium on Computer Applications and Industrial Electronics*, pp. 100–104, Oct. 2015, doi: 10.1109/ISCAIE.2015.7298336.
- [56] C. M. Affonso, W. Freitas, W. Xu, and L. C. P. da Silva, "Performance of ROCOF relays for embedded generation applications," *IEE Proceedings: Generation, Transmission and Distribution*, vol. 152, no. 1, pp. 109–114, Jan. 2005, doi: 10.1049/IP-GTD:20041079.

- [57] W. Freitas, W. Xu, C. M. Affonso, and Z. Huang, “Comparative analysis between ROCOF and vector surge relays for distributed generation applications,” *IEEE Transactions on Power Delivery*, vol. 20, no. 2 II, pp. 1315–1324, Apr. 2005, doi: 10.1109/TPWRD.2004.834869.
- [58] M. R. Alam, M. T. A. Begum, and K. M. Muttaqi, “Assessing the Performance of ROCOF Relay for Anti-Islanding Protection of Distributed Generation under Subcritical Region of Power Imbalance,” *IEEE Transactions on Industry Applications*, vol. 55, no. 5, pp. 5395–5405, Sep. 2019, doi: 10.1109/TIA.2019.2927667.
- [59] M. A. Redfern, O. Usta, and G. Fielding, “Protection against loss of utility grid supply for a dispersed storage and generation unit,” *IEEE Transactions on Power Delivery*, vol. 8, no. 3, pp. 948–954, 1993, doi: 10.1109/61.252622.
- [60] M. el Azzaoui, “Islanding Detection Method with Load Power Factor Improvement and High Frequency Transient Suppressing,” *IEEE Transactions on Smart Grid*, vol. 12, no. 5, pp. 4176–4184, Sep. 2021, doi: 10.1109/TSG.2021.3080306.
- [61] M. Grebla, J. R. A. K. Yellajosula, and H. K. Hoidalén, “Adaptive Frequency Estimation Method for ROCOF Islanding Detection Relay,” *IEEE Transactions on Power Delivery*, vol. 35, no. 4, pp. 1867–1875, Aug. 2020, doi: 10.1109/TPWRD.2019.2956200.
- [62] C. Li, C. Cao, Y. Cao, Y. Kuang, L. Zeng, and B. Fang, “A review of islanding detection methods for microgrid,” *Renewable and Sustainable Energy Reviews*, vol. 35, pp. 211–220, Jul. 2014, doi: 10.1016/J.RSER.2014.04.026.
- [63] O. N. Faqhruldin, E. F. El-Saadany, and H. H. Zeineldin, “A universal islanding detection technique for distributed generation using pattern recognition,” *IEEE Transactions on Smart Grid*, vol. 5, no. 4, pp. 1985–1992, 2014, doi: 10.1109/TSG.2014.2302439.

- [64] A. Khamis, Y. Xu, Z. Y. Dong, and R. Zhang, “Faster Detection of Microgrid Islanding Events Using an Adaptive Ensemble Classifier,” *IEEE Transactions on Smart Grid*, vol. 9, no. 3, pp. 1889–1899, May 2018, doi: 10.1109/TSG.2016.2601656.
- [65] P. Du, Z. Ye, E. E. Aponte, J. K. Nelson, and L. Fan, “Positive-feedback-based active anti-islanding schemes for inverter-based distributed generators: Basic principle, design guideline and performance analysis,” *IEEE Transactions on Power Electronics*, vol. 25, no. 12, pp. 2941–2948, 2010, doi: 10.1109/TPEL.2010.2057446.
- [66] X. Wang and W. Freitas, “Impact of positive-feedback anti-islanding methods on small-signal stability of inverter-based distributed generation,” *IEEE Transactions on Energy Conversion*, vol. 23, no. 3, pp. 923–931, 2008, doi: 10.1109/TEC.2008.926066.
- [67] J. R. Kan, N. Li, Z. L. Yao, Y. C. Xue, and D. C. Wu, “Anti-islanding performance of grid-connected inverters based on frequency droop PLL,” *Conference Proceedings - 2012 IEEE 7th International Power Electronics and Motion Control Conference - ECCE Asia, IPEMC 2012*, vol. 3, pp. 2129–2133, 2012, doi: 10.1109/IPEMC.2012.6259174.
- [68] I.-Y. Chung and S.-I. Moon, “A New Islanding Detection Method using Phase-Locked Loop for Inverter-Interfaced Distributed Generators,” *Journal of Electrical Engineering and Technology*, vol. 2, no. 2, pp. 165–171, Jun. 2007, doi: 10.5370/JEET.2007.2.2.165.
- [69] H. Lahiji, F. Badrkhani Ajaei, and R. E. Boudreau, “Non-Pilot Protection of the Inverter- Dominated Microgrid,” *IEEE Access*, vol. 7, pp. 142190–142202, 2019, doi: 10.1109/ACCESS.2019.2944137.
- [70] H. Lahiji, “Non-Pilot Protection of the Inverter-Dominated AC Microgrid,” *Electronic Thesis and Dissertation Repository*, Sep. 2018, Accessed: Nov. 16, 2022. [Online]. Available: <https://ir.lib.uwo.ca/etd/5748>

- [71] T. K. Abdel-Galil *et al.*, “Protection coordination planning with distributed generation,” *Qualsys Engco. Inc*, 2007.
- [72] “929-2000 - IEEE Recommended Practice for Utility Interface of Photovoltaic (PV) Systems | IEEE Standard | IEEE Xplore.”
- [73] S. Dutta, P. K. Sadhu, M. Jaya Bharata Reddy, and D. K. Mohanta, “Shifting of research trends in islanding detection method - a comprehensive survey,” *Protection and Control of Modern Power Systems*, vol. 3, no. 1, Dec. 2018, doi: 10.1186/S41601-017-0075-8.
- [74] M. Ciobotaru, V. G. Agelidis, R. Teodorescu, and F. Blaabjerg, “Accurate and less-disturbing active antiislanding method based on pll for grid-connected converters,” *IEEE Transactions on Power Electronics*, vol. 25, no. 6, pp. 1576–1584, 2010, doi: 10.1109/TPEL.2010.2040088.
- [75] P. Gupta, R. S. Bhatia, and D. Jain, “A hybrid technique for islanding detection of an inverter based distributed generation,” *2012 IEEE 5th Power India Conference, PICONF 2012*, 2012, doi: 10.1109/POWERI.2012.6479535.
- [76] M. E. Ropp, M. Begovic, A. Rohatgi, G. A. Kern, R. H. Bonn, and S. Gonzalez, “Determining the relative effectiveness of islanding detection methods using phase criteria and nondetection zones,” *IEEE Transactions on Energy Conversion*, vol. 15, no. 3, pp. 290–296, Sep. 2000, doi: 10.1109/60.875495.
- [77] A. Serrano-Fontova, J. A. Martinez, P. Casals-Torrens, and R. Bosch, “A robust islanding detection method with zero-non-detection zone for distribution systems with DG,” *International Journal of Electrical Power & Energy Systems*, vol. 133, p. 107247, Dec. 2021, doi: 10.1016/J.IJEPES.2021.107247.
- [78] W. Bower and M. Ropp, “Evaluation of Islanding Detection Methods for Photovoltaic Utility-Interactive Power Systems Task V, Report IEAPVPS T5-09, Mar. 2002.” 2000.

- [79] A. Khamis, H. Shareef, E. Bizkevelci, and T. Khatib, "A review of islanding detection techniques for renewable distributed generation systems," *Renewable and Sustainable Energy Reviews*, vol. 28, pp. 483–493, Dec. 2013, doi: 10.1016/J.RSER.2013.08.025.
- [80] K. N. E. Ku Ahmad, J. Selvaraj, and N. A. Rahim, "A review of the islanding detection methods in grid-connected PV inverters," *Renewable and Sustainable Energy Reviews*, vol. 21, pp. 756–766, May 2013, doi: 10.1016/J.RSER.2013.01.018.
- [81] M. Vatani, T. Amraee, and I. Soltani, "Comparative of Islanding Detection Passive Methods for Distributed Generation Applications," *International Journal of Innovation and Scientific Research*, vol. 8, no. 2, pp. 234–241, 2014, Accessed: Aug. 24, 2022. [Online]. Available: <http://www.ijisr.issr-journals.org/>
- [82] A. Makkieh *et al.*, "Assessment of passive islanding detection methods for DC microgrids," *IET Conference Publications*, vol. 2019, no. CP751, 2019, doi: 10.1049/CP.2019.0016.
- [83] T. Funabashi, K. Koyanagi, and R. Yokoyama, "A review of islanding detection methods for distributed resources," *2003 IEEE Bologna PowerTech - Conference Proceedings*, vol. 2, pp. 608–613, 2003, doi: 10.1109/PTC.2003.1304617.
- [84] J. C. M. Vieira, W. Freitas, Z. Huang, W. Xu, and A. Morelato, "Formulas for predicting the dynamic performance of ROCOF relays for embedded generation applications," *IEE Proceedings: Generation, Transmission and Distribution*, vol. 153, no. 4, pp. 399–406, Jul. 2006, doi: 10.1049/IP-GTD:20045205.
- [85] J. C. M. Vieira, W. Freitas, W. Xu, and A. Morelato, "Performance of frequency relays for distributed generation protection," *IEEE Transactions on Power Delivery*, vol. 21, no. 3, pp. 1120–1127, Jul. 2006, doi: 10.1109/TPWRD.2005.858751.

- [86] A. B. Piardi, R. B. Otto, L. Otremba, D. Motter, A. P. G. Pavani, and R. A. Ramos, “Impact of ROCOF-based islanding detection on the stand-alone operation of a distributed synchronous generator,” *2019 IEEE Milan PowerTech, PowerTech 2019*, Jun. 2019, doi: 10.1109/PTC.2019.8810844.
- [87] M. Yu and Y. Zhao, “A Novel Frequency-RoCoF Islanding Detection Method for Grid-connected Distributed Generation,” *5th IEEE Conference on Energy Internet and Energy System Integration: Energy Internet for Carbon Neutrality, EI2 2021*, pp. 1374–1378, 2021, doi: 10.1109/EI252483.2021.9713617.
- [88] J. A. Cebollero, D. Cañete, S. Martín-Arroyo, M. García-Gracia, and H. Leite, “A Survey of Islanding Detection Methods for Microgrids and Assessment of Non-Detection Zones in Comparison with Grid Codes,” *Energies 2022, Vol. 15, Page 460*, vol. 15, no. 2, p. 460, Jan. 2022, doi: 10.3390/EN15020460.
- [89] R. de C. Fernandez and H. Rojas, “An overview of wavelet transforms application in power systems,” in *Proc. 14th PSSC*, 2002, pp. 1–8. Accessed: Aug. 28, 2022. [Online]. Available: http://www.uta.cl/hdiaz/Papers/An_overview_of_wavelet_transform_applications_in_power_systems.pdf
- [90] S. Suja and J. Jerome, “Pattern recognition of power signal disturbances using S Transform and TT Transform,” *International Journal of Electrical Power & Energy Systems*, vol. 32, no. 1, pp. 37–53, Jan. 2010, doi: 10.1016/J.IJEPES.2009.06.012.
- [91] P. K. Ray, N. Kishor, and S. R. Mohanty, “Islanding and Power Quality Disturbance Detection in Grid-Connected Hybrid Power System Using Wavelet and S-Transform,” *IEEE Transactions on Smart Grid*, vol. 3, no. 3, pp. 1082–1094, Sep. 2012, doi: 10.1109/TSG.2012.2197642.
- [92] N. W. A. Lidula and A. D. Rajapakse, “A pattern-recognition approach for detecting power islands using transient signals-part II: Performance evaluation,”

IEEE Transactions on Power Delivery, vol. 27, no. 3, pp. 1071–1080, 2012, doi: 10.1109/TPWRD.2012.2187344.

- [93] N. W. A. Lidula and A. D. Rajapakse, “A pattern recognition approach for detecting power islands using transient signals - Part I: Design and implementation,” *IEEE Transactions on Power Delivery*, vol. 25, no. 4, pp. 3070–3077, Oct. 2010, doi: 10.1109/TPWRD.2010.2053724.
- [94] S. Raza, H. Mokhlis, H. Arof, J. A. Laghari, and L. Wang, “Application of signal processing techniques for islanding detection of distributed generation in distribution network: A review,” *Energy Convers Manag*, vol. 96, pp. 613–624, May 2015, doi: 10.1016/J.ENCONMAN.2015.03.029.
- [95] A. Ashrafiyan, M. Rostami, and G. B. Gharehpetian, “Hyperbolic S-transform-based method for classification of external faults, incipient faults, inrush currents and internal faults in power transformers,” *IET Generation, Transmission and Distribution*, vol. 6, no. 10, pp. 940–950, Oct. 2012, doi: 10.1049/IET-GTD.2012.0047.
- [96] Z. K. Peng, P. W. Tse, and F. L. Chu, “An improved Hilbert–Huang transform and its application in vibration signal analysis,” *J Sound Vib*, vol. 286, no. 1–2, pp. 187–205, Aug. 2005, doi: 10.1016/J.JSV.2004.10.005.
- [97] N. E. Huang *et al.*, “The empirical mode decomposition and the Hilbert spectrum for nonlinear and non-stationary time series analysis,” *Proceedings of the Royal Society A: Mathematical, Physical and Engineering Sciences*, vol. 454, no. 1971, pp. 903–995, Mar. 1998, doi: 10.1098/RSPA.1998.0193.
- [98] D. Donnelly, “The Fast Fourier and Hilbert-Huang Transforms: A Comparison,” pp. 84–88, Aug. 2007, doi: 10.1109/CESA.2006.4281628.
- [99] A. Y. Ayenu-Prah and N. O. Attah-Okine, “Comparative study of Hilbert–Huang transform, Fourier transform and wavelet transform in pavement profile analysis,”

<http://dx.doi.org/10.1080/00423110802167466>, vol. 47, no. 4, pp. 437–456, Apr. 2009, doi: 10.1080/00423110802167466.

- [100] Z. K. Peng, P. W. Tse, and F. L. Chu, “A comparison study of improved Hilbert–Huang transform and wavelet transform: Application to fault diagnosis for rolling bearing,” *Mech Syst Signal Process*, vol. 19, no. 5, pp. 974–988, Sep. 2005, doi: 10.1016/J.YMSSP.2004.01.006.
- [101] A. H. Mohammadzadeh Niaki and S. Afsharnia, “A new passive islanding detection method and its performance evaluation for multi-DG systems,” *Electric Power Systems Research*, vol. 110, pp. 180–187, May 2014, doi: 10.1016/J.EPSR.2014.01.016.
- [102] J. M. Ha, J. M. Lee, J. H. Lee, D. S. Gu, and B. K. Choi, “Signal processing method (HT and HHT) of AE for complex fault detection,” *Materials Science Forum*, vol. 762, pp. 656–661, 2013, doi: 10.4028/WWW.SCIENTIFIC.NET/MSF.762.656.
- [103] B. K. Chaitanya, A. Yadav, M. Pazoki, and A. Y. Abdelaziz, “A comprehensive review of islanding detection methods,” *Uncertainties in Modern Power Systems*, pp. 211–256, Jan. 2021, doi: 10.1016/B978-0-12-820491-7.00008-6.
- [104] S. R. Mohanty, N. Kishor, P. K. Ray, and J. P. S. Catalao, “Comparative study of advanced signal processing techniques for islanding detection in a hybrid distributed generation system,” *IEEE Transactions on Sustainable Energy*, vol. 6, no. 1, pp. 122–131, Jan. 2015, doi: 10.1109/TSTE.2014.2362797.
- [105] M. A. Farhan and K. Shanti Swarup, “Mathematical morphology-based islanding detection for distributed generation,” *IET Generation, Transmission & Distribution*, vol. 10, no. 2, pp. 518–525, Feb. 2016, doi: 10.1049/IET-GTD.2015.0910.

- [106] R. A. Peters, "A New Algorithm for Image Noise Reduction Using Mathematical Morphology," *IEEE Transactions on Image Processing*, vol. 4, no. 5, pp. 554–568, 1995, doi: 10.1109/83.382491.
- [107] I. Q. Butt, S. A. A. Kazmi, S. B. Ali Bukhari, and S. Ahmad, "Passive islanding detection using square law method," *2021 International Conference on Emerging Power Technologies, ICEPT 2021*, Apr. 2021, doi: 10.1109/ICEPT51706.2021.9435493.
- [108] R. Haider *et al.*, "Passive islanding detection scheme based on autocorrelation function of modal current envelope for photovoltaic units," *IET Generation, Transmission & Distribution*, vol. 12, no. 3, pp. 726–736, Feb. 2018, doi: 10.1049/IET-GTD.2017.0823.
- [109] R. Bakhshi-Jafarabadi, J. Sadeh, A. Serrano-Fontova, and E. Rakhshani, "Review on islanding detection methods for grid-connected photovoltaic systems, existing limitations and future insights," *IET Renewable Power Generation*, Nov. 2022, doi: 10.1049/RPG2.12554.
- [110] M. Liserre, A. Pigazo, A. Dell'Aquila, and V. M. Moreno, "An anti-islanding method for single-phase inverters based on a grid voltage sensorless control," *IEEE Transactions on Industrial Electronics*, vol. 53, no. 5, pp. 1418–1426, Oct. 2006, doi: 10.1109/TIE.2006.882003.
- [111] A. A. Girgis and T. L. Daniel, "Optimal estimation of voltage phasors and frequency deviation using linear and non-linear kalman filtering: Theory and limitations," *IEEE Transactions on Power Apparatus and Systems*, vol. PAS-103, no. 10, pp. 2943–2951, 1984, doi: 10.1109/TPAS.1984.318297.
- [112] R. Aghazadeh, H. Lesani, M. Sanaye-Pasand, and B. Ganji, "New technique for frequency and amplitude estimation of power system signals," *IEE Proceedings: Generation, Transmission and Distribution*, vol. 152, no. 3, pp. 435–440, May 2005, doi: 10.1049/IP-GTD:20041255.

- [113] B. Panomruttanarug and R. Longman, “The advantages and disadvantages of kalman filtering in repetitive control,” in *Advances in the Astronautical Sciences*, 2008. Accessed: Nov. 17, 2022. [Online]. Available: https://www.researchgate.net/publication/290710523_The_advantages_and_disadvantages_of_kalman_filtering_in_repetitive_control
- [114] S. Admasie, S. B. A. Bukhari, T. Gush, R. Haider, and C. H. Kim, “Intelligent Islanding Detection of Multi-distributed Generation Using Artificial Neural Network Based on Intrinsic Mode Function Feature,” *Journal of Modern Power Systems and Clean Energy*, vol. 8, no. 3, pp. 511–520, May 2020, doi: 10.35833/MPCE.2019.000255.
- [115] H. Samet, F. Hashemi, and T. Ghanbari, “Minimum non detection zone for islanding detection using an optimal Artificial Neural Network algorithm based on PSO,” *Renewable and Sustainable Energy Reviews*, vol. 52, pp. 1–18, Dec. 2015, doi: 10.1016/J.RSER.2015.07.080.
- [116] S. Raza, H. Mokhlis, H. Arof, K. Naidu, J. A. Laghari, and A. S. M. Khairuddin, “Minimum-features-based ANN-PSO approach for islanding detection in distribution system,” *IET Renewable Power Generation*, vol. 10, no. 9, pp. 1255–1263, Oct. 2016, doi: 10.1049/IET-RPG.2016.0080.
- [117] V. L. Merlin, R. C. Santos, A. P. Grilo, J. C. M. Vieira, D. v. Coury, and M. Oleskovicz, “A new artificial neural network based method for islanding detection of distributed generators,” *International Journal of Electrical Power & Energy Systems*, vol. 75, pp. 139–151, Feb. 2016, doi: 10.1016/J.IJEPES.2015.08.016.
- [118] M. S. ElNozahy, E. F. El-Saadany, and M. M. A. Salama, “A robust wavelet-ANN based technique for islanding detection,” *IEEE Power and Energy Society General Meeting*, 2011, doi: 10.1109/PES.2011.6039158.
- [119] N. W. A. Lidula, N. Perera, and A. D. Rajapakse, “Investigation of a fast islanding detection methodology using transient signals,” *2009 IEEE Power and Energy Society General Meeting, PES '09*, 2009, doi: 10.1109/PES.2009.5275780.

- [120] S. R. Samantaray, B. C. Babu, and P. K. Dash, "Probabilistic Neural Network Based Islanding Detection in Distributed Generation," <http://dx.doi.org/10.1080/15325008.2010.526986>, vol. 39, no. 3, pp. 191–203, Jan. 2011, doi: 10.1080/15325008.2010.526986.
- [121] A. Y. Hatata, E. H. Abd-Raboh, and B. E. Sedhom, "Proposed Sandia frequency shift for anti-islanding detection method based on artificial immune system," *Alexandria Engineering Journal*, vol. 57, no. 1, pp. 235–245, Mar. 2018, doi: 10.1016/J.AEJ.2016.12.020.
- [122] G. Yin, "A distributed generation islanding detection method based on artificial immune system," *Proceedings of the IEEE Power Engineering Society Transmission and Distribution Conference*, vol. 2005, pp. 1–4, 2005, doi: 10.1109/TDC.2005.1547072.
- [123] R. Azim *et al.*, "A decision tree based approach for microgrid islanding detection," *2015 IEEE Power and Energy Society Innovative Smart Grid Technologies Conference, ISGT 2015*, Jun. 2015, doi: 10.1109/ISGT.2015.7131809.
- [124] M. Heidari, G. Seifossadat, and M. Razaz, "Application of decision tree and discrete wavelet transform for an optimized intelligent-based islanding detection method in distributed systems with distributed generations," *Renewable and Sustainable Energy Reviews*, vol. 27, pp. 525–532, Nov. 2013, doi: 10.1016/J.RSER.2013.06.047.
- [125] R. Sun, Z. Wu, and V. A. Centeno, "Power system islanding detection & identification using topology approach and decision tree," *IEEE Power and Energy Society General Meeting*, 2011, doi: 10.1109/PES.2011.6039088.
- [126] M. S. Thomas and P. P. Terang, "Islanding detection using decision tree approach," *2010 Joint International Conference on Power Electronics, Drives and Energy Systems, PEDES 2010 and 2010 Power India*, 2010, doi: 10.1109/PEDES.2010.5712394.

- [127] H. Shayeghi, B. Sobhani, E. Shahryari, and A. Akbarimajd, "Optimal neuro-fuzzy based islanding detection method for Distributed Generation," *Neurocomputing*, vol. 177, pp. 478–488, Feb. 2016, doi: 10.1016/J.NEUCOM.2015.11.056.
- [128] H. Bitaraf, M. Sheikholeslamzadeh, A. M. Ranjbar, and B. Mozafari, "Neuro-fuzzy islanding detection in distributed generation," *2012 IEEE Innovative Smart Grid Technologies - Asia, ISGT Asia 2012*, 2012, doi: 10.1109/ISGT-ASIA.2012.6303292.
- [129] F. Hashemi, N. Ghadimi, and B. Sobhani, "Islanding detection for inverter-based DG coupled with using an adaptive neuro-fuzzy inference system," *International Journal of Electrical Power and Energy Systems*, vol. 45, no. 1, pp. 443–455, Feb. 2013, doi: 10.1016/J.IJEPES.2012.09.008.
- [130] N. Ghadimi, "An adaptive neuro-fuzzy inference system for islanding detection in wind turbine as distributed generation," *Complexity*, vol. 21, no. 1, pp. 10–20, Sep. 2015, doi: 10.1002/CPLX.21537.
- [131] S. R. Samantaray, K. El-Arroudi, G. Joós, and I. Kamwa, "A fuzzy rule-based approach for islanding detection in distributed generation," *IEEE Transactions on Power Delivery*, vol. 25, no. 3, pp. 1427–1433, Jul. 2010, doi: 10.1109/TPWRD.2010.2042625.
- [132] A. G. Abd-Elkader, D. F. Allam, and E. Tageldin, "Islanding detection method for DFIG wind turbines using artificial neural networks," *International Journal of Electrical Power & Energy Systems*, vol. 62, pp. 335–343, Nov. 2014, doi: 10.1016/J.IJEPES.2014.04.052.
- [133] N. W. A. Lidula and A. D. Rajapakse, "Fast and reliable detection of power islands using transient signals," *ICIIS 2009 - 4th International Conference on Industrial and Information Systems 2009, Conference Proceedings*, pp. 493–498, 2009, doi: 10.1109/ICIINFS.2009.5429812.

- [134] S. S. Madani, A. Abbaspour, M. Beiraghi, P. Z. Dehkordi, and A. M. Ranjbar, "Islanding detection for PV and DFIG using decision tree and AdaBoost algorithm," *IEEE PES Innovative Smart Grid Technologies Conference Europe*, 2012, doi: 10.1109/ISGTEUROPE.2012.6465818.
- [135] T. Wang, Z. Li, Y. Yan, and H. Chen, "A survey of fuzzy decision tree classifier methodology," *Advances in Soft Computing*, vol. 40, pp. 959–968, 2007, doi: 10.1007/978-3-540-71441-5_104.
- [136] P. K. Dash, M. Padhee, and T. K. Panigrahi, "A hybrid time–frequency approach based fuzzy logic system for power island detection in grid connected distributed generation," *International Journal of Electrical Power & Energy Systems*, vol. 42, no. 1, pp. 453–464, Nov. 2012, doi: 10.1016/J.IJEPES.2012.04.003.
- [137] S. Mohamadian, H. Pairo, and A. Ghasemian, "A Straightforward Quadrature Signal Generator for Single-Phase SOGI-PLL with Low Susceptibility to Grid Harmonics," *IEEE Transactions on Industrial Electronics*, vol. 69, no. 7, pp. 6997–7007, Jul. 2022, doi: 10.1109/TIE.2021.3095813.
- [138] M. S. Reza, F. Sadeque, M. M. Hossain, A. M. Y. M. Ghias, and V. G. Agelidis, "Three-phase pll for grid-connected power converters under both amplitude and phase unbalanced conditions," *IEEE Transactions on Industrial Electronics*, vol. 66, no. 11, pp. 8881–8891, Nov. 2019, doi: 10.1109/TIE.2019.2893857.
- [139] G. C. Hsieh and J. C. Hung, "Phase-locked loop techniques - A survey," *IEEE Transactions on Industrial Electronics*, vol. 43, no. 6, pp. 609–615, 1996, doi: 10.1109/41.544547.
- [140] T. Thacker, D. Boroyevich, R. Burgos, and F. Wang, "Phase-locked loop noise reduction via phase detector implementation for single-phase systems," *IEEE Transactions on Industrial Electronics*, vol. 58, no. 6, pp. 2482–2490, Jun. 2011, doi: 10.1109/TIE.2010.2069070.

- [141] D. Dong, B. Wen, D. Boroyevich, P. Mattavelli, and Y. Xue, “Analysis of phase-locked loop low-frequency stability in three-phase grid-connected power converters considering impedance interactions,” *IEEE Transactions on Industrial Electronics*, vol. 62, no. 1, pp. 310–321, Jan. 2015, doi: 10.1109/TIE.2014.2334665.
- [142] A. A. Ahmad, M. Pichan, and A. Abrishamifar, “A new simple structure PLL for both single and three phase applications,” *International Journal of Electrical Power & Energy Systems*, vol. 74, pp. 118–125, Jan. 2016, doi: 10.1016/J.IJEPES.2015.07.021.
- [143] T. Thacker, F. Wang, R. Burgos, and D. Boroyevich, “Islanding detection using a coordinate transformation based phase-locked loop,” *PESC Record - IEEE Annual Power Electronics Specialists Conference*, pp. 1151–1156, 2007, doi: 10.1109/PESC.2007.4342155.

Appendices

Appendix A: Study System 1 Parameters

The general parameters, line lengths, and load specifications of study system 1 are provided in the tables below.

Table A.1: General System Parameters – Study System 1.

Component	Description
Grid	$V_{LL-base} = 27.6 \text{ kV}, 60 \text{ Hz}$ $S_{nom} = 20 \text{ MVA}, SSC = 885.33, X/R = 10$
Wind power plant	$S_{WT} = 4 \text{ MVA} = 2 \times 2 \text{ MVA}$
PV power plant	$S_{PV} = 3.5 \text{ MVA}$
BESS units	$S_{BESS} = 2 \times 2 \text{ MVA}$
Transformers	T1: 3.6 MVA, 6% impedance, 27.6 kV/8.31 kV, ΔY T2: 15 MVA, 7.3% impedance, 27.6 kV/27.6 kV, YY T3: 1 MVA, 4% impedance, 27.6 kV/8.31 kV, ΔY T4: 3.6 MVA, 5.65% impedance, 27.6 kV/8.31 kV, ΔY
Overhead lines	Spacing ID = STD-3PH-NBP, $R_l = 0.172 \text{ } \Omega/\text{km}, R_0 = 0.491 \text{ } \Omega/\text{km},$ $X_l = 0.404 \text{ } \Omega/\text{km}, X_0 = 1.354 \text{ } \Omega/\text{km},$ $B_l = 4.171 \text{ uS/km}, B_0 = 1.759 \text{ uS/km}$

Table A.2: Overhead Lines Lengths – Study System 1.

Line	Length (m)	Line	Length (m)	Line	Length (m)
L1	5700	L11	3330	L21	1550
L2	1010	L12	1030	L22	2120
L3	400	L13	3490	L23	1820
L4	380	L14	1430	L24	2540
L5	120	L15	190	L25	620
L6	170	L16	1940	L26	3580
L7	260	L17	2450	L27	770
L8	140	L18	1630	L28	2080
L9	940	L19	1200	L29	4510
L10	300	L20	820	L30	4040

Table A.3: Load Specifications – Study System 1¹.

Load #	Three Phase KVA	Power Factor
1	2364	0.95
2	346	0.87
3	3355	0.95
4	256	0.75
5	6.3	1
6	265	0.95
7	650	1
8	50	0.95
9	160	0.95
10	205	1
11	445	0.95
12	10	0.95
13	215	0.95
14	85	0.95
15	110	0.95

¹ Load #16 is a special load described in part 4.2.4 and does not exist in the original system.

Appendix B: Study System 3 Parameters

The general parameters, load specifications, and parameters of the hardware-implemented converters of study system 3 are provided in the tables below.

Table A.4: General System Parameters – Study System 3.

Transformer		750 VA, 7% impedance, 208 V/160 V, YY
Lines	L1	$R = 25 \text{ m}\Omega, L = 56 \text{ }\mu\text{H}, C = 20 \text{ nF}$
	L2	$R = 50 \text{ m}\Omega, L = 120 \text{ }\mu\text{H}, C = 33 \text{ nF}$
	L3	$R = 25 \text{ m}\Omega, L = 120 \text{ }\mu\text{H}, C = 0.56 \text{ nF}$
	L4	$R = 10 \text{ m}\Omega, L = 176 \text{ }\mu\text{H}, C = 1.2 \text{ nF}$
	L5	$R = 50 \text{ m}\Omega, L = 200 \text{ }\mu\text{H}, C = 1 \text{ nF}$

Table A.5: Load Specifications – Study System 3.

DC-L1	10 W DC
DC-L2	10 W DC
AC-L1	10 W AC
AC-L2	10 W AC
AC-L3	30 W AC

Table A.6: DC/DC Converter Specifications – Study System 3.

Rated power	80 W
Rated input DC voltage	40 V
Filter inductance	150.0 μ H
DC filter capacitance	20 μ F
Switching frequency	48 kHz

Table A.7: AC/DC VSC Specifications – Study System 3.

Rated power	90 W
Rated DC link voltage	40 V
LCL filter inverter-side inductance	300 μ H
LCL filter capacitance	50 μ F
LCL filter grid-side inductance	21.7 μ H
LCL filter damping resistance	0.75 Ω
DC link filter capacitance	20 μ F
Switching frequency	18 kHz

Table A.8: Battery Specifications.

Rated voltage	2 \times 12 V DC
Capacity	2 \times 10 Ah

Curriculum Vitae

Name: Hoda Zamani

Post-Secondary Education and Degrees: Amirkabir University of Technology
(Tehran Polytechnic)
Tehran, Iran
2015-2019 B.Sc. in Electrical Engineering

Honours and Awards: Hydro One Graduate Scholarship
2022

Identified as *Exceptional Talented Student* by National Organization for Development of Exceptional Talents (NODET)
2019, 2015

Ranked 1st among the power systems students
Amirkabir University of Technology
(Tehran Polytechnic)
2019

Related Work Experience: Teaching Assistant
Western University
2016-2017, 2018-2019, 2021-now

Vice-president at Graduate Engineering Society (GES)
Western University
2021